

---

# Robust Asymmetric Learning in POMDPs

---

Andrew Warrington<sup>\*1</sup> J. Wilder Lavington<sup>\*2,3</sup> Adam Ścibior<sup>2,3</sup> Mark Schmidt<sup>2,4</sup> Frank Wood<sup>2,3,5</sup>

## Abstract

Policies for partially observed Markov decision processes can be efficiently learned by imitating expert policies generated using asymmetric information. Unfortunately, existing approaches for this kind of imitation learning have a serious flaw: the expert does not know what the trainee cannot see, and as a result, may encourage actions that are sub-optimal or unsafe under partial information. To address this issue, we derive an update which, when applied iteratively to an expert, maximizes the expected reward of the trainee’s policy. Using this update, we construct a computationally efficient algorithm, adaptive asymmetric DAgger (A2D), that jointly trains the expert and trainee policies. We then show that A2D allows the trainee to safely imitate the modified expert, and outperforms policies learned either by imitating a fixed expert or through direct reinforcement learning.

## 1. Introduction

Consider the stochastic shortest path problem (Bertsekas & Tsitsiklis, 1991) where an agent learns to cross a frozen lake while avoiding patches of weak ice. The agent can either cross the ice directly, or take the longer, safer route circumnavigating the lake. The agent is provided with aerial images of the lake, which includes color variations at patches of weak ice. To cross the lake, the agent must learn to identify its own position, goal position, and the locations of weak ice from the images. Even for this simple environment, high-dimensional inputs and sparse rewards can make learning a suitable policy computationally expensive and sample inefficient. Therefore one might instead efficiently learn, in simulation, an omniscient *expert*, conditioned on a low-dimensional vector which fully describes the state of the world, to complete the task. A *trainee*, observing only images, can then learn to mimic the

actions of the expert using sample-efficient online imitation learning (Ross et al., 2011). This yields a high-performing trainee, conditioned on images, learned with fewer environment interactions overall compared to direct reinforcement learning (RL).

While appealing, this approach can fail in environments where the expert has access to information unavailable to the agent, referred to as *asymmetric information*. Consider instead that the image of the lake does not indicate the location of the weak ice. The trainee now operates under uncertainty, resulting in a different optimal policy. However, imitating the expert forces the trainee to always cross the lake, despite being unable to locate and avoid the weak ice. Even though the expert is optimal under full information, the supervision provided to the trainee through imitation learning is poor and yields a policy that is not optimal under partial information. The key insight is that *the expert has no knowledge of what the trainee does not know*. Therefore the expert cannot provide suitable supervision, and proposes actions that are not robust to the increased uncertainty under partial information. The main algorithmic contribution we present follows from this insight: the *expert* must be refined based on the behavior of the *trainee* imitating it.

Building on this insight, we present a new algorithm: adaptive asymmetric DAgger (A2D), illustrated in Figure 1. Our algorithm enhances conventional imitation learning by refining the expert policy, such that the resulting supervision moves the trainee policy closer to the optimal *partially observed* policy. This allows us to safely take advantage of asymmetric information in imitation learning. Crucially, A2D can be easily integrated with a variety of different RL algorithms, does not require any pre-trained artifacts, policies or example trajectories, and does not take computationally expensive and high-variance reinforcement learning steps in the trainee’s policy network.

We first frame asymmetric imitation learning (AIL) as utilizing full state information from the corresponding Markov decision process (MDP) to efficiently supervise policy learning in a partially observed Markov decision process (POMDP). We then formalize this solution as an approximate posterior inference problem. Using this connection, we define a sufficient condition for when the expert will provide correct supervision to the trainee. We then derive the A2D expert

---

<sup>\*</sup>Equal contribution <sup>1</sup>Department of Engineering Science, University of Oxford <sup>2</sup>Department of Computer Science, University of British Columbia <sup>3</sup>inverted.ai <sup>4</sup>Alberta Machine Learning Intelligence Institute (AMII) <sup>5</sup>Montréal Institute for Learning Algorithms (MILA).

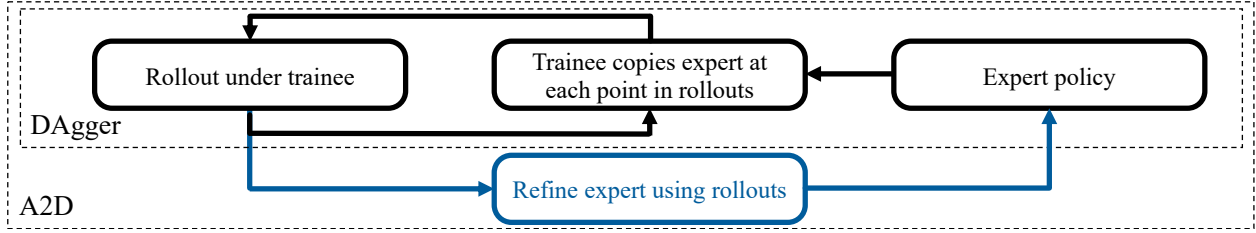


Figure 1: Flow chart describing adaptive asymmetric DAGger (A2D) introduced in this work, which builds on DAGger (Ross et al., 2011) by further refining the expert conditioned on the trainee’s policy.

policy gradient update, by composing the posterior described above with the partially observed RL objective, and differentiating with respect to the parameters of the expert policy. To verify these expert’s gradient updates improve the learned trainee’s performance, we experiment with two grid world environments and an autonomous vehicle scenario. We find that A2D recovers the optimal partially observed policy with fewer samples, lower computational cost, and less variance. These experiments demonstrate the efficacy of A2D, and makes learning via imitation and reinforcement safer and more efficient, even in difficult high dimensional control problems such as autonomous driving.

## 2. Background

### 2.1. Optimality & MDPs

An MDP,  $\mathcal{M}_\Theta(\mathcal{S}, \mathcal{A}, \mathcal{R}, \mathcal{T}_0, \mathcal{T}, \Pi_\Theta)$ , is defined as a random process which produces a sequence  $\tau_t := \{a_t, s_t, s_{t+1}, r_t\}$ , for a set of states  $s_t \in \mathcal{S}$ , actions  $a_t \in \mathcal{A}$ , initial state  $p(s_0) \in \mathcal{T}_0$ , transition dynamics  $p(s_{t+1}|s_t, a_t) \in \mathcal{T}$ , reward function  $r_t : \mathcal{S} \times \mathcal{A} \times \mathcal{S} \rightarrow \mathbb{R}$ , and policy  $\pi_\theta \in \Pi_\Theta : \mathcal{S} \rightarrow \mathcal{A}$  parameterized by  $\theta \in \Theta$ . The generative model, shown in Figure 2, for a finite horizon process is defined as:

$$q_{\pi_\theta}(\tau) = p(s_0) \prod_{t=0}^T p(s_{t+1}|s_t, a_t) \pi_\theta(a_t|s_t). \quad (1)$$

We denote the marginal distribution over state  $s_t \in \mathcal{S}$  at time  $t$  as  $q_{\pi_\theta}(s_t)$ . The objective of RL is to recover the policy which maximizes the expected cumulative reward over a trajectory,  $\theta^* = \arg \max_{\theta \in \Theta} \mathbb{E}_{q_{\pi_\theta}} [\sum_{t=0}^T r_t(s_t, a_t, s_{t+1})]$ . This paper considers an extension of this framework, where we instead maximize the non-stationary, infinite horizon discounted return. This optimization problem is defined as:

$$\theta^* = \max_{\theta \in \Theta} \mathbb{E}_{s \sim d^{\pi_\theta}, a \sim \pi_\theta} [Q^{\pi_\theta}(a, s)], \quad (2)$$

$$\text{where } d^{\pi_\theta}(s) = (1 - \gamma) \sum_{t=0}^{\infty} \gamma^t q_{\pi_\theta}(s_t = s), \quad (3)$$

$$Q^{\pi_\theta}(a, s) = \mathbb{E}_{\substack{p(s', a, s') \\ p_\theta(a'|s')}} \left[ r(s, a, s') + \gamma \mathbb{E}_{\pi_\theta} [Q^{\pi_\theta}(a', s')] \right], \quad (4)$$

where  $d^{\pi_\theta}(s)$  is referred to as the *state occupancy* (Agarwal et al., 2020), and the *Q function*,  $Q^\pi$ , defines the expected

discounted sum of rewards ahead given a particular state-action pair.

### 2.2. State Estimation and POMDPs

A POMDP extends an MDP by observing a random variable  $o_t \in \mathcal{O}$ , dependent on the state,  $o_t \sim p(\cdot|s_t)$ , instead of the state itself. The policy then samples actions conditioned on all previous observations and actions:  $\pi_\phi(a_t|a_{0:t-1}, o_{0:t})$ . In practice, a belief state statistic  $b_t \in \mathcal{B}$  is constructed from  $a_{0:t-1}, o_{0:t}$ , as an estimate of the underlying state, on which the policy is conditioned, sampling actions from  $\pi_\phi \in \Pi_\Phi : \mathcal{B} \rightarrow \mathcal{A}$  (Doshi-Velez et al., 2013; Igl et al., 2018; Kaelbling et al., 1998). The resulting stochastic process, denoted  $\mathcal{M}_\Phi(\mathcal{S}, \mathcal{O}, \mathcal{B}, \mathcal{A}, \mathcal{R}, \mathcal{T}_0, \mathcal{T}, \Pi_\Phi)$ , generates a sequence of tuples  $\tau_t = \{a_t, b_t, o_t, s_t, s_{t+1}, r_t\}$ . As before, we wish to find a policy,  $\pi_{\phi^*} \in \Pi_\Phi$ , which maximizes the expected cumulative reward under the generative model:

$$q_{\pi_\phi}(\tau) = p(s_0) \prod_{t=0}^T p(s_{t+1}|s_t, a_t) \times p(b_t|b_{t-1}, o_t, a_{t-1}) p(o_t|s_t) \pi_\phi(a_t|b_t). \quad (5)$$

It is common practice to condition on the last  $w$  observations and actions (Laskin et al., 2020a; Murphy, 2000), i.e.  $b_t := (a_{t-w:t-1}, o_{t-w:t})$ , rather than using the potentially infinite dimensional random variable (Murphy, 2000), defined recursively in Figure 2. Throughout this paper,  $q_\pi$  is used to denote the distribution over trajectories under the policy in the subscript (Equations (1) and (5) for  $\pi_\theta(\cdot|s_t)$  and  $\pi_\phi(\cdot|b_t)$  respectively). Similarly, the occupancies  $d^{\pi_\phi}(s)$  and  $d^{\pi_\phi}(b)$  define marginals of  $d^{\pi_\phi}(s, b)$  in a partially observed processes (as in Equation (3)). Later we discuss *MDP-POMDP pairs*, which we define as an MDP and a POMDP with identical state transition dynamics, reward generating functions and initial state distributions. However, these process pairs can, and often do, have different optimal policies. This discrepancy is the central issue addressed in this work.

### 2.3. Imitation Learning

Imitation learning (IL) assumes access to either an expert policy capable of solving a task, or example trajectories generated by such an expert. Given example trajectories, the

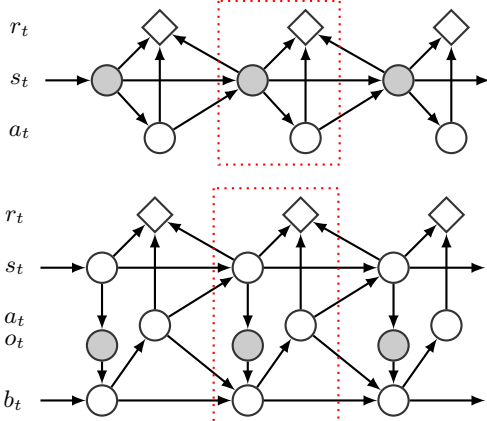


Figure 2: Graphical models of an MDP (top) and a POMDP (bottom) with identical initial and state transition dynamics,  $p(s_t|s_{t-1}, a_t)$ ,  $p(s_0)$ , and reward function  $R(s_t, a_t, s_{t+1})$ .

*trainee* is learned via regressing onto the actions of the expert. However, this approach can perform arbitrarily poorly for states not in the training set (Laskey et al., 2017). Alternatively, online IL (OIL) algorithms, such as DAgger (Ross et al., 2011), assume access to an expert that can be queried at any state. DAgger interacts with the environment under a mixture of the expert  $\pi_\theta$  and trainee  $\pi_\phi$  policies, denoted  $\pi_\beta$ , then updates the trainee to replicate experts’ actions:

$$\phi^* = \arg \min_{\phi} \mathbb{E}_{d^{\pi_\beta}(s)} [\mathbb{KL}[\pi_\theta(a|s) || \pi_\phi(a|s)]], \quad (6)$$

$$\text{where } \pi_\beta(a|s) = \beta\pi_\theta(a|s) + (1 - \beta)\pi_\phi(a|s). \quad (7)$$

The coefficient  $\beta$  is annealed to zero during training, which ensures supervision in states likely visited by the trainee, thereby avoiding compounding out of distribution error which grows with time-horizon (Ross et al., 2011; Sun et al., 2017). While IL provides higher sample efficiency than RL, it requires an expert or expert trajectories, and is thus not always applicable. Crucially, for an imperfect expert, a trainee learned via IL can perform arbitrarily poorly (Sun et al., 2017), even in the OIL setting. The addition of asymmetry in OIL leads to similar failures.

## 2.4. Asymmetric Information

In many simulated environments, additional information is available during training that is not available at test time. This additional *asymmetric information* can often be exploited to accelerate learning (Choudhury et al., 2018; Pinto et al., 2017; Vapnik & Vashist, 2009). For example, Pinto et al. (2017) exploit asymmetry to learn to control a robotic arm. In this paper, the policy is conditioned on noisy image-based observations which are available at test time. The value function (or *critic*) however, is conditioned on a compact and noiseless state representation of joint positions and velocities, only available during training. The objective for this *asymmetric*

*actor critic* (Pinto et al., 2017) algorithm is:

$$J(\phi) = \mathbb{E}_{d^{\pi_\phi}(s,b)} \left[ \mathbb{E}_{\pi_\phi(a|b)} [A^{\pi_\phi}(s,a)] \right], \quad (8)$$

$$Q^{\pi_\phi}(a,s) = \mathbb{E}_{p(s'|s,a)} [r(s,a,s') + \gamma V^{\pi_\phi}(s')], \quad (9)$$

$$V^{\pi_\phi}(s) = \mathbb{E}_{\pi_\phi(a|b)} [Q^{\pi_\phi}(a,s)], \quad (10)$$

where the *asymmetric advantage* is defined as  $A^{\pi_\phi}(s,a) = Q^{\pi_\phi}(a,s) - V^{\pi_\phi}(s)$ , and  $V^{\pi_\phi}(s)$  is the *asymmetric value function*. These methods often outperform “symmetric” RL as  $Q^{\pi_\phi}(a,s)$  and  $V^{\pi_\phi}(s)$  are simpler to tune, train, and provide lower-variance gradient estimates.

Asymmetric information has also been used in a variety of other scenarios, including policy ensembles (Sasaki & Yamashina, 2021; Song et al., 2019), imitating attention-based representations (Salter et al., 2019), multi-objective RL (Schwab et al., 2019), direct state reconstruction (Nguyen et al., 2020), or through privileged information dropout (Kamienny et al., 2020; Lambert et al., 2018). We note that failures induced by asymmetric information are also discussed in works by Arora et al. (2018) and Choudhury et al. (2018). Arora et al. (2018) identify a particular scenario where a particular method fails. Choudhury et al. (2018) use asymmetric information to improve policy optimization in model predictive control, but note that their solution does not address scenarios such as “the trapped robot problem,” which we refer to as the tiger door problem (Littman et al., 1995), and tackle later on.

Asymmetric environments are also naturally suited to OIL, referred to as asymmetric OIL (AIL) (Pinto et al., 2017):

$$\phi^* = \arg \min_{\phi} \mathbb{E}_{d^{\pi_\beta}(s,b)} [\mathbb{KL}[\pi_\theta(a|s) || \pi_\phi(a|b)]],$$

$$\text{where } \pi_\beta(a|s,b) = \beta\pi_\theta(a|s) + (1 - \beta)\pi_\phi(a|b). \quad (11)$$

As the expert is not used at test time, AIL can take advantage of asymmetry to simplify learning (Pinto et al., 2017) or enable data augmentation (Chen et al., 2020). However, naive application of AIL can yield trainees that perform arbitrarily poorly. Work has addressed learning from imperfect experts Ross & Bagnell (2014); Sun et al. (2017); Meng et al. (2019), but does not consider issues arising from the use of asymmetric information. We demonstrate, analyze, and then remedy this failure in the following sections.

## 3. AIL as Posterior Inference

We begin by analyzing the AIL objective in Equation (11). We show the optimal trainee defined by this objective is also defined by the solution to a posterior inference problem over state that depends on the expert policy. This definition will allow us to reason more easily about how the parameters of the expert policy affects the learned trainee, and will help us derive an update to the expert that enables recovery of the

optimal POMDP policy through imitation. We first define the posterior inference problem solved by a trainee as:

**Definition 1** (Implicit policy). *For any state-conditional policy  $\pi_\theta \in \hat{\Pi}_\Theta$  and any belief-conditional policy  $\pi_\eta \in \hat{\Pi}_\Phi$  we define  $\hat{\pi}_\theta^\eta \in \hat{\Pi}_\Theta$*

$$\hat{\pi}_\theta^\eta(a|b) := \mathbb{E}_{s_t \sim d^{\pi_\eta}(s|b)} [\pi_\theta(a|s)], \quad (12)$$

as the implicit policy of  $\pi_\theta$  under  $\pi_\eta$ . When  $\pi_\eta = \hat{\pi}_\theta^\eta$ , we refer to the latter as the implicit policy of  $\pi_\theta$ , written as  $\hat{\pi}_\theta$ .

The implicit policy represents a posterior predictive density which averages over the uncertainty associated with the underlying state distribution. This posterior defines the solution to the AIL objective in Equation (11) (when  $\beta = 0$ ):

**Theorem 1** (Asymmetric IL target). *For any fully observing policy  $\pi_\theta$  and fixed policy  $\pi_\eta$ , the implicit policy  $\hat{\pi}_\theta^\eta$ , defined in Definition 1, minimizes the asymmetric IL objective:*

$$\hat{\pi}_\theta^\eta = \arg \min_{\pi \in \Pi_\Phi} \mathbb{E}_{d^{\pi_\eta}(s,b)} [\mathbb{KL}[\pi_\theta(a|s) || \pi(a|b)]]. \quad (13)$$

*Proof.* An extended proof is included in Appendix C.

$$\begin{aligned} & \mathbb{E}_{d^{\pi_\eta}(s,b)} [\mathbb{KL}[\pi_\theta(a|s) || \pi(a|b)]] \\ &= \mathbb{E}_{d^{\pi_\eta}(b)} \left[ \mathbb{E}_{d^{\pi_\eta}(s)(a|b)} \left[ \mathbb{E}_{\pi_\theta(a|s)} [\log \pi(a|b)] \right] \right] + K \\ &= \mathbb{E}_{d^{\pi_\eta}(b)} \left[ \mathbb{E}_{a \sim \hat{\pi}_\theta^\eta} [\log \pi(a|b)] \right] + K \\ &= \mathbb{E}_{d^{\pi_\eta}(b)} [\mathbb{KL}[\hat{\pi}_\theta^\eta(a|b) || \pi(a|b)]] + K' \end{aligned}$$

Since  $\hat{\pi}_\theta^\eta \in \Pi_\Phi$ , it follows that

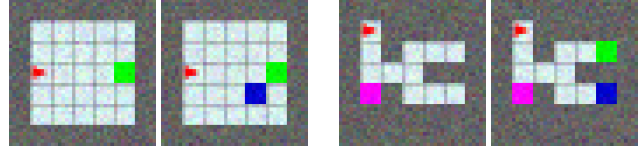
$$\begin{aligned} \hat{\pi}_\theta^\eta &= \arg \min_{\pi \in \Pi_\Phi} \mathbb{E}_{d^{\pi_\eta}(b)} [\mathbb{KL}[\hat{\pi}_\theta^\eta(a|b) || \pi(a|b)]] \\ &= \arg \min_{\pi \in \Pi_\Phi} \mathbb{E}_{d^{\pi_\eta}(s,b)} [\mathbb{KL}[\pi_\theta(a|s) || \pi(a|b)]]. \quad \square \end{aligned} \quad (14)$$

Because sampling from  $d^{\pi_\eta}(s|b)$  is intractable, sampling from the implicit policy is also intractable. Therefore, AIL learns a variational approximation  $\pi_\psi \in \Pi_\psi : \mathcal{B} \rightarrow \mathcal{A}$  to the implicit policy by minimizing the following objective:

$$F(\psi) = \mathbb{E}_{d^{\pi_\eta}(s,b)} [\mathbb{KL}[\pi_\theta(a|s) || \pi_\psi(a|b)]], \quad (15)$$

$$\nabla_\psi F(\psi) = -\mathbb{E}_{d^{\pi_\eta}(s,b)} \left[ \mathbb{E}_{\pi_\theta(a|s)} [\nabla_\psi \log \pi_\psi(a|b)] \right]. \quad (16)$$

Unlike Equation (12), this objective avoids sampling from the *conditional* occupancy, instead sampling from the joint occupancy. If the variational family is sufficiently expressive, there exists a  $\pi_\psi \in \Pi_\psi$  for which the divergence between the implicit policy and the variational approximation is zero. In OIL, it is common to sample under the trainee policy by setting  $\pi_\eta = \pi_\psi$ , thereby defining a fixed point equation. Under sufficient expressivity and exact optimization steps, the iteration converges to the implicit policy (see Appendix C). In practice, we also find that this iterative scheme converges, even in the presence of inexact optimization steps.



(a) Frozen lake.

(b) Tiger door.

Figure 3: Two gridworlds we study. An agent (red) must navigate to the goal (green) while avoiding the hazard (blue). The expert is conditioned on an omniscient compact state vector indicating the position of the goal and hazard. In “frozen lake”, the trainee is conditioned on the left image and cannot see the hazard. In “tiger door”, pushing the button (pink) illuminates the hazard (blue).

## 4. Failure of Asymmetric Imitation Learning

Now that we have defined the AIL solution, we can reason about when AIL itself might fail. We show a class of failure cases rooted in implicit policies, and hence variational policies, with a non-zero divergence to the expert. In this environment class, the trainee policy can incur arbitrarily low reward, even if the expert is optimal under full information. To explore this we first introduce two scenarios from this environment class, where the divergence is non-zero, and AIL fails. We then identify a condition that guarantees AIL will succeed. This condition informs how the expert can be modified to ensure the optimal partially observed policy is recovered.

We explore two gridworld environments, referred to as “frozen lake” and “tiger door” (Littman et al., 1995; Spaan, 2012), illustrated in Figure 3. Both require an agent (red) to navigate to a goal while avoiding hazards. The trainee is conditioned on an image of the environment where the hazard is not initially visible, while the expert is conditioned on an omniscient compact state vector. Every action incurs a base reward of  $-2$ , reaching the goal earns a reward of  $20$ , and hitting the hazard incurs a reward of  $-50$ . In frozen lake, the hazard (weak ice) is in a random location in the interior nine squares. In tiger door, the agent can push a button, incurring a negative reward as a result of extra actions, to reveal to goal position.

Results for these environments, shown in Figure 4, confirm our intuitions: Learning the expert using RL in the MDP (denoted RL (MDP)) is stable and efficient. The expert proceeds directly to the goal, earning rewards of  $10.66$  and  $6$  respectively. Direct RL in the POMDP (denoted RL and RL (Asym)) is slow and inefficient, and does not converge to a performant policy. The trainee policy learned using AIL converges almost immediately. However, this policy averages over expert actions and proceeds straight across the ice in frozen lake, or, directly to a possible goal location in tiger door, incurring rewards of  $-26.6$  and  $-54$  respectively. Both

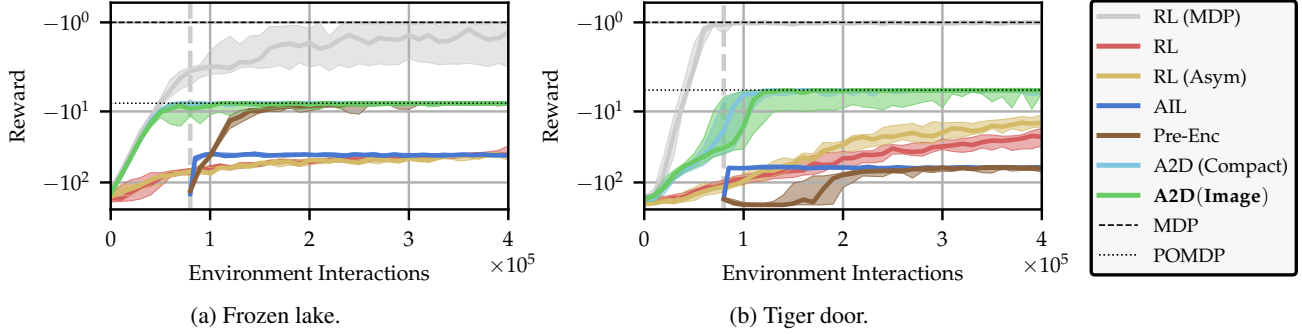


Figure 4: Results for the gridworld environments. Median and quartiles across 25 random seeds are shown. TRPO (Schulman et al., 2015a) is used for RL methods. Broken lines indicate the optimal reward, normalized so the optimal MDP reward is  $-1$  (MDP). All agents and trainees are conditioned on a partial image-based input, except *A2D (Compact)* which is conditioned on a partial compact state representation (i.e. an optimal manually specified image encoding, indicating only the position of the trainee, and the position of the goal and hazard once the button is pushed). All experts, and *RL (MDP)*, are conditioned on an omniscient compact state, and are not valid agents themselves. *Pre-Enc* uses a fixed pretrained encoder, trained on examples from the MDP, which converts an image into a compact state estimate. *AIL* and *Pre-Enc* begin when the MDP has converged, as this is the required expenditure for training. *A2D* is the only method reliably and efficiently finds the optimal POMDP policy in a sample budget commensurate with *RL (MDP)*. The convergence of *A2D* is also similar for both image-based (*A2D (Image)*) and compact (*A2D (Compact)*) representations, highlighting that we have effectively subsumed the image perception task. Configurations, additional results and discussions are included in the appendix.

of these solutions represent catastrophic failures. Instead, the trainee should circumnavigate the lake, or, push the button and then proceed to the goal pose, earning rewards of 4 and 2 respectively.

These results, and insight from Theorem 1, lead us to define a property of an MDP-POMDP policy and process pair:

**Definition 2** (Identifiable Policies and Processes). *Given an MDP  $\mathcal{M}_\Theta$  and POMDP  $\mathcal{M}_\Phi$  pair, with MDP policy  $\pi_\theta \in \Pi_\Theta$  and implicit policy  $\hat{\pi}_\theta \in \hat{\Pi}_\Theta$ , we describe  $\{\pi_\theta, \hat{\pi}_\theta\}$  as an **identifiable policy pair** if and only if  $\mathbb{E}_{d^{\hat{\pi}_\theta}(s,b)} [\mathbb{KL}[\pi_\theta(a|s) | \hat{\pi}_\theta(a|b)]] = 0$ . If this condition holds for all  $\pi_\theta \in \Pi_{\Theta^*}$ , we define the MDP-POMDP process pair  $\{\mathcal{M}_\Theta, \mathcal{M}_\Phi\}$  as a **identifiable process pair**.*

A result then follows for an identifiable process pair:

**Theorem 2** (Convergence of AIL). *For any identifiable process pair defined over sufficiently expressive model classes, under exact intermediate updates, iteration defined by:*

$$\psi_{k+1} = \arg \min_{\psi \in \Psi} \mathbb{E}_{d^{\pi_{\psi_k}}(s,b)} [\mathbb{KL}[\pi_{\theta^*}(a|s) | \pi_\psi(a|b)]], \quad (17)$$

where  $\pi_{\theta^*}(a|s)$  defines the optimal policy under full information, converges to the optimal partially observed policy  $\pi_{\psi^*}(a|b)$  as  $k \rightarrow \infty$ .

*Proof.* See Appendix C.  $\square$

Crucially, the expert policy is only guaranteed to provide correct supervision and recover the optimal agent policy for identifiable process pairs. When this condition is not satisfied, as in the gridworlds above, the learned policy can be

arbitrarily sub-optimal. However this is a fixed property of an MDP-POMDP pair, too restrictive to be satisfied by most environments. We therefore propose a new approach that instead modifies the expert, such that the modified expert policy and corresponding implicit policy pair form an identifiable policy pair, and, that the corresponding implicit policy is equal to the optimal partially observing policy. This allows asymptotically correct supervision and ensures the optimal trainee is recovered through application of AIL.

## 5. Correcting AIL with Expert Refinement

We now use the insight from Sections 3 and 4 to construct an update, applied to the expert policy, which improves the expected reward ahead under the implicit policy. Crucially, this update is designed such that, when interleaved with AIL, the optimal partially observed policy is recovered. We refer to this iterative algorithm as adaptive asymmetric DAgger (A2D). To derive an update to the expert  $\pi_\theta$ , we first consider the RL objective under the corresponding implicit policy  $\hat{\pi}_\theta$ :

$$J(\theta) = \mathbb{E}_{d^{\hat{\pi}_\theta}(b) \hat{\pi}_\theta(a|b)} [Q^{\hat{\pi}_\theta}(a, b)], \quad \text{where} \quad (18)$$

$$Q^{\hat{\pi}_\theta}(a, b) = \mathbb{E}_{p(b', s' | a, b)} \left[ r(s, a, s') + \gamma \mathbb{E}_{\hat{\pi}_\theta(a' | b')} [Q^{\hat{\pi}_\theta}(a', b')] \right].$$

This objective defines the cumulative reward of the trainee in terms of the parameters of the expert policy. This means that maximizing  $J(\theta)$ , maximizes the reward obtained by the implicit policy, and ensures proper expert supervision:

**Theorem 3** (Convergence of Exact A2D). *Under exact intermediate updates, the following iteration converges to an*

optimal partially observed policy  $\pi_{\psi^*}(a_t|b_t) \in \Pi_\phi$ , provided both  $\Pi_{\phi^*} \subseteq \hat{\Pi}_{\theta^*} \subseteq \Pi_\psi$  for some  $\pi_\theta \in \Pi_\theta$ :

$$\psi_{k+1} = \arg \min_{\psi \in \Psi} \mathbb{E}_{d^{\pi_{\psi_k}(s,b)}} [\mathbb{KL} [\pi_{\hat{\theta}^*}(a|s) || \pi_\psi(a|b)]], \quad (19)$$

$$\text{where } \hat{\theta}^* = \arg \max_{\theta \in \Theta} \mathbb{E}_{d^{\pi_{\psi_k}(b)\hat{\pi}_\theta(a|b)}} [Q^{\hat{\pi}_\theta}(a, b)]. \quad (20)$$

*Proof.* See Appendix C  $\square$

However, directly operating on  $Q^{\hat{\pi}_\theta}$  is intractable as sampling from  $\hat{\pi}_\theta$  is intractable. Instead, to update the expert, we use a surrogate objective, denoted  $J_\psi(\theta)$ , which replaces  $Q^{\hat{\pi}_\theta}$  with the expected reward under the variational agent policy  $Q^{\pi_\psi}$ . By maximizing this surrogate objective, we maximize a lower bound on the possible improvement to the implicit policy with respect to the experts parameters:

$$\max_{\theta} J_\psi(\theta) = \max_{\theta} \mathbb{E}_{\hat{\pi}_\theta(a|b)d^{\pi_\psi(b)}} [Q^{\pi_\psi}(a, b)] \quad (21)$$

$$\leq \max_{\theta} \mathbb{E}_{\hat{\pi}_\theta(a|b)d^{\pi_\psi(b)}} [Q^{\hat{\pi}_\theta}(a, b)] = \max_{\theta} J(\theta). \quad (22)$$

Replacement with a *behavioral policy*, here  $\pi_\psi$ , is a common analysis technique, especially in policy gradient (Schulman et al., 2015a; 2017; Sutton, 1992) and policy search methods (see §4,5 of Bertsekas (2019) and §2 of Deisenroth et al. (2013)). For more discussion see Appendix C. This surrogate objective permits the following REINFORCE gradient estimator, where we define  $\nabla_\theta f_\theta = \nabla_\theta \log \pi_\theta(a|s)$ :

$$\nabla_\theta J_\psi(\theta) = \nabla_\theta \mathbb{E}_{\hat{\pi}_\theta(a|b), d^{\pi_\psi(b)}} [Q^{\pi_\psi}(a, b)], \quad (23)$$

$$\begin{aligned} &= \mathbb{E}_{d^{\pi_\psi(b)}} \left[ \nabla_\theta \mathbb{E}_{d^{\pi_\psi(s|b)}} \left[ \mathbb{E}_{\pi_\theta(a|s)} [Q^{\pi_\psi}(a, b)] \right] \right], \\ &= \mathbb{E}_{d^{\pi_\psi(s,b)}} \left[ \mathbb{E}_{\pi_\theta(a|s)} [Q^{\pi_\psi}(a, b) \nabla_\theta f_\theta] \right], \\ &= \mathbb{E}_{d^{\pi_\psi(s,b)} \pi_\psi(a|b)} \left[ \frac{\pi_\theta(a|s)}{\pi_\psi(a|b)} Q^{\pi_\psi}(a, b) \nabla_\theta f_\theta \right]. \quad (24) \end{aligned}$$

To guarantee this estimator is unbiased, the Q function must be learned directly. However, in many environments, explicitly learning the Q function can be avoided. In practice we find using Monte Carlo Q function estimates provides faster and more reliable convergence. A performance gap and non-zero policy divergence present simple indicators that an explicit Q function is, or is not, required. A detailed investigation of this and additional experimental results are included in Appendix B.

Similar to DAgger, A2D interacts under a mixture policy  $\pi_\beta(a|s, b) = \beta\pi_\theta(a|s) + (1 - \beta)\pi_\psi(a|b)$ , with Q and value function defined as  $Q^{\pi_\beta}(a, s, b)$  and  $V^{\pi_\beta}(a, s, b)$  respectively. The mixture coefficient  $\beta$  is annealed from one to

---

**Algorithm 1** Adaptive Asymmetric DAgger (A2D)
 

---

- 1: **Input:** MDP  $\mathcal{M}_\theta$ , POMDP  $\mathcal{M}_\phi$ , Annealing schedule  $\text{AnnealBeta}(n, \beta)$ .
  - 2: **Return:** Variational policy parameters  $\psi$ .
  - 3:  $\theta, \psi, \nu_m, \nu_p \leftarrow \text{InitNets}(\mathcal{M}_\theta, \mathcal{M}_\phi)$
  - 4:  $\beta \leftarrow 1, D \leftarrow \emptyset$
  - 5: **for**  $n = 0, \dots, N$  **do**
  - 6:    $\beta \leftarrow \text{AnnealBeta}(n, \beta)$
  - 7:    $\pi_\beta \leftarrow \beta\pi_\theta + (1 - \beta)\hat{\pi}_\psi$
  - 8:    $\mathcal{T} = \{\tau_i\}_{i=1}^T \sim q_{\pi_\beta}(\tau)$
  - 9:    $D \leftarrow \text{UpdateBuffer}(D, \mathcal{T})$
  - 10:    $V^{\pi_\beta} \leftarrow \beta V^{\pi_\theta} + (1 - \beta)V^{\hat{\pi}_\psi}$
  - 11:    $\theta, \nu_m, \nu_p \leftarrow \text{RLStep}(\mathcal{T}, V^{\pi_\beta}, \pi_\beta)$
  - 12:    $\psi \leftarrow \text{AILStep}(D, \pi_\theta, \hat{\pi}_\psi)$
  - 13: **end for**
- 

Algorithm 1: The adaptive asymmetric DAgger (A2D) algorithm we introduce. The additional steps we introduce beyond DAgger (Ross et al., 2011) are highlighted in blue, and implement the additional feedback loop in Figure 1. `RLStep` is a policy gradient step, updating the expert, using the gradient estimator in Equation (25). `AILStep` is an AIL variational policy update, as in Equation (16).

zero during training. The final Monte Carlo gradient estimator (using GAE (Schulman et al., 2015b)) is given as:

$$\nabla_\theta J_\psi(\theta) = \mathbb{E}_{\substack{d^{\pi_\beta(s_t, b_t)} \\ \pi_\beta(a_t|s_t, b_t)}} \left[ \frac{\pi_\theta(a_t|s_t) \hat{A}^{\pi_\beta} \nabla_\theta f_\theta}{\pi_\beta(a_t|s_t, b_t)} \right], \quad (25)$$

$$\text{where } \hat{A}^{\pi_\beta}(a_t, s_t, b_t) = \sum_{t=0}^{\infty} (\gamma\lambda)^t \delta_t, \quad (26)$$

$$\text{and } \delta_t = r_t + \gamma V^{\pi_\beta}(s_{t+1}, b_{t+1}) - V^{\pi_\beta}(s_t, b_t). \quad (27)$$

We can now define the A2D algorithm, shown in Algorithm 1. A2D first interacts with the environment, applies the A2D update to the expert policy, and then performs an AIL step:

1. **Gather data** (Alg. 1, Ln 8): Collect samples by rolling out under the mixture policy by sampling trajectories from  $q_{\pi_\beta}(\tau)$  as defined in Equation (5).
2. **Refine Expert** (Alg. 1, Ln 11): Apply policy gradient step to the expert with importance weighted advantage as per Equation (25). This step updates the expert policy parameters,  $\theta$ , trainee value function parameters,  $\nu_p$ , and expert value function parameters,  $\nu_m$ .
3. **Update Trainee** (Alg. 1, Ln 12): Perform an AIL step to fit the (variational) trainee policy parameters,  $\psi$ , to the expert policy using Equation (16).

The A2D update is simply an importance weighted policy gradient step, and hence is compatible with any REINFORCE-based policy gradient methods, such as TRPO or PPO (Schulman et al., 2015a; 2017) (see Appendix B).

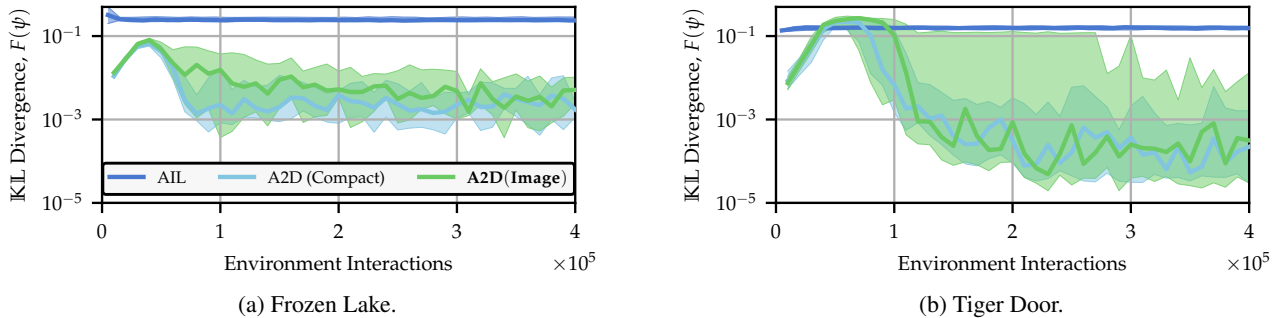


Figure 5: The evolution of the policy divergence,  $F(\psi)$ . Shown are the median and quartiles across 25 random seeds. *AIL* converges to a high divergence, whereas *A2D* achieves a low divergence for both representations, indicating that the trainee is faithfully imitating the expert, and recovers by *A2D* (see Figure 4 for more information).

## 6. Experiments

### 6.1. Revisiting Frozen Lake & Tiger Door

We now evaluate *A2D* on the gridworlds introduced in Section 3. These results are included in Figures 4 and 5. We see in Figure 4 that *A2D* converges to the optimal POMDP reward in a similar number of environment interactions as the best-possible convergence (*RL (MDP)*), whereas the other methods fail for one, or both, gridworlds. Crucially, this convergence is observed when both high-dimensional images (*A2D (Image)*), and low-dimensional compact representations (*A2D (Compact)*), are used as agent inputs.

Figure 5 shows the divergence between the expert and trainee policies during learning. *AIL* saturates to a high divergence, indicating that the trainee is unable to replicate the expert. The divergence in *A2D* increases initially, as the expert learns quickly while  $\beta$  is high, and then decreases as  $\beta$  decays and the expert is forced to optimize just the reward of the trainee. The divergence approaches zero as expert and trainee policies successfully coalesce. Therefore, *A2D* has successfully created an identifiable expert and implicit policy pair, as per Definition 2, where this implicit policy is equal to the optimal partially observing policy, as predicted by Theorem 2 and empirically validated in Figure 4.

### 6.2. Safe Autonomous Vehicle Learning

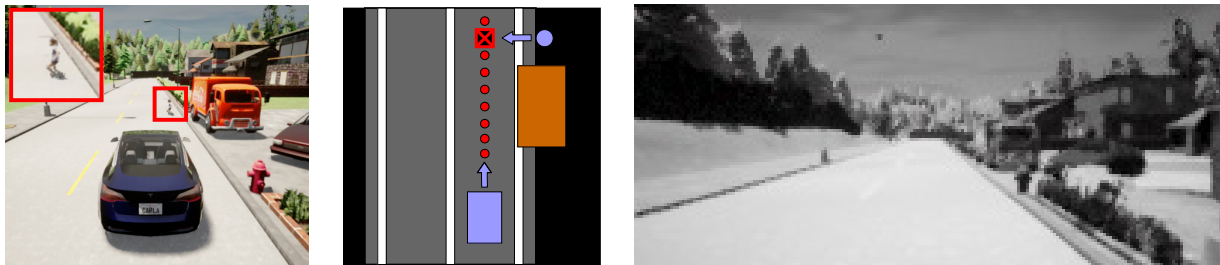
Autonomous vehicle (AV) simulators (Dosovitskiy et al., 2017; Wymann et al., 2014; Kato et al., 2015), allow safe virtual exploration of driving scenarios that would be unsafe to explore in real life. The inherent complexity of training AV controllers makes exploiting efficient *AIL* an attractive opportunity (Chen et al., 2020). The expert can be provided with the exact state of other actors, such as other vehicles, occluded hazards and traffic lights. The trainee is provided with sensor measurements only available in the real world, such as camera feeds, lidar and the egovehicle telemetry.

The safety-critical aspects of asymmetry are even clearer

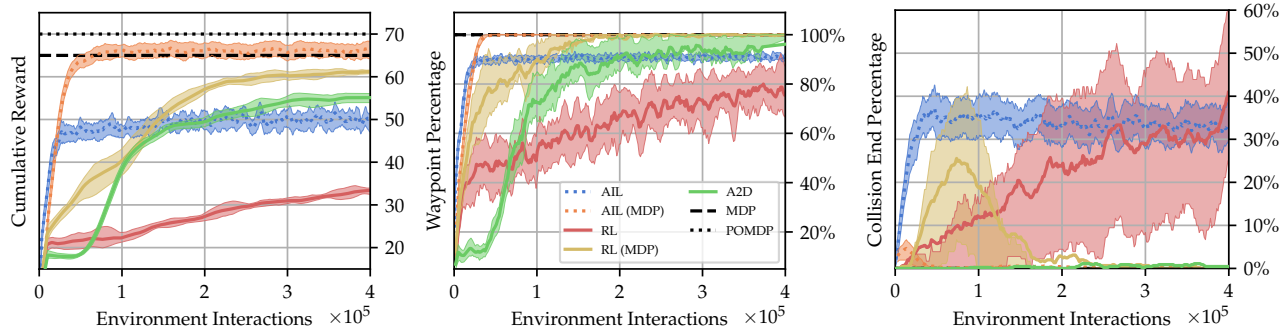
in context of AVs. Consider a scenario where a child may or may not run into the road from behind a parked truck, illustrated in Figure 6a. The expert, aware of the position and velocity of the child from asymmetric information, will only brake if there is a child, and will otherwise proceed at high speed. However, the trainee is unable to distinguish between these scenarios from just the front-facing camera feed. As the expected expert behavior is to accelerate, the implicit agent policy will also accelerate, only starting to braking once the child is visible by which time it is too late. The agent should therefore proceed at a lower speed so it can slow down or evade the child once visible. This cannot be achieved by naive application of *AIL*.

We implement this scenario in the CARLA simulator (Dosovitskiy et al., 2017). A child is present in 50% of trials, and, if present, emerges with variable velocity. The action space consists of the steering angle and amount of throttle/brake. The differentiable expert is a small neural network, operating on a six dimensional compact-state vector that fully describes the simulator state. The agent is a convolutional neural network that operates on a grayscale image from the forward facing camera, shown in Figure 6a. As an approximation to the optimal policy under privileged information, we used a hand-coded expert that completes the scenario driving at the speed limit if the child is absent, and slows down when approaching the truck if the child is present.

We benchmark *A2D* against four baselines, presented in Figure 6b. *RL (MDP)* learns an agent conditioned on the compact state, only available in simulation, using RL. This represents the unrealistic best-case performance without manual specification, achieving good, although not optimal, performance reasonably quickly and reliably. *RL* learns an agent conditioned on the camera image, achieving poor, high-variance results within our experimental budget. *AIL* uses asymmetric *DAgger* to imitate the hand-coded expert using the camera image. It learns quickly, but converges to a solution with a high collision rate due to relying on unsafe supervision. For completeness we include *AIL (MDP)*, which



(a) Visualizations of the AV scenario. Left: third-person view showing the ego vehicle and the child running out. Center: top-down schematic view of the environment showing the asymmetric information available. Right: front-view camera input provided to the agent.



(b) Performance metrics for the AV scenario. We show mean and quartiles across ten random seeds. Left: average cumulative reward. Center: average percentage of waypoints collected, measuring progress along the route. Right: percentage of trajectories ending in collision, which indicates hitting the child. The optimal MDP and POMDP solutions are given by the dashed and dotted lines respectively.

Figure 6: Visualizations and results for the AV scenario introduced in Section 6. In methods marked as MDP the agent uses an omniscient compact state vector, and hence removes the perception problem and has knowledge of the child before emergence from behind the truck. Therefore AIL (*AIL (MDP)*) and RL (*RL (MDP)*) learn a performant (high reward and waypoint percentage, low collision percentage) policy quickly and reliably. In methods marked as POMDP the agent uses the high-dimensional image representation, and hence is unaware of the child. Therefore AIL (*AIL*) leads to collisions (high collision percentage), while the perception problem makes RL in the POMDP (*RL*) slow and variable (low reward, waypoint percentage, and high collision percentage). Our A2D algorithm (*A2D*) solves the scenario (high reward, and waypoint percentage, low collision percentage) in a budget commensurate with the omniscient compact state expert (*RL (MDP)*).

learns a policy conditioned on the omniscient state by imitating a hand-coded expert, and converges very quickly to the near optimal solution (*MDP*). As expected, we find that *A2D* learns slower than the AIL variants, since RL is used to update to the expert, but eventually achieves higher reward than *AIL* while avoiding most collisions.

## 7. Discussion

In this work we discuss learning policies in POMDPs, where partial information and high-dimensional observations makes direct application of RL expensive and unreliable. Asymmetric learning uses additional information, available in simulation, to improve performance beyond comparable symmetric learning methods. Asymmetric IL can efficiently learn a partially observing policy by imitating an omniscient expert, but requires a pre-existing expert, and, critically, assumes that the expert can provide suitable supervision — a condition we formalize as identifiability. When this condition is not

satisfied, the learned agent can perform arbitrarily poorly. We therefore develop adaptive asymmetric DAGger (*A2D*), which adapts the expert policy such that AIL can efficiently recover the optimal partially observed policy. *A2D* also allows the expert to be learned online with the agent and does not require any pretrained artifacts. We then demonstrate that *A2D* outperforms a number of alternative approaches.

We believe that *A2D* is in fact complementary to other existing methods. If the observed dimension is small, direct application of RL is likely to perform well and reliably. If the observed dimension is large and a pretrained expert is available, AIL provides an efficient approach, but may fail catastrophically. If examples are available that cover the state-space visited by the optimal agent policy then using a pretrained encoder can yield a low-overhead approach. Notably, *A2D* makes none of these assumptions, is robust, and expedites training in asymmetric environments.



## 8. Acknowledgements

We thank Frederik Kunstner for his invaluable discussions, and for reviewing preliminary drafts of this work. Andrew Warrington is supported by the Shilston Scholarship, Keble College, University of Oxford. J. Wilder Lavington is supported by Inverted AI. We acknowledge the support of the Natural Sciences and Engineering Research Council of Canada (NSERC), the Canada CIFAR AI Chairs Program, and the Intel Parallel Computing Centers program. This material is based upon work supported by the United States Air Force Research Laboratory (AFRL) under the Defense Advanced Research Projects Agency (DARPA) Data Driven Discovery Models (D3M) program (Contract No. FA8750-19-2-0222) and Learning with Less Labels (LwLL) program (Contract No. FA8750-19-C-0515). Additional support was provided by UBC's Composites Research Network (CRN), Data Science Institute (DSI) and Support for Teams to Advance Interdisciplinary Research (STAIR) Grants. This research was enabled in part by technical support and computational resources provided by WestGrid (<https://www.westgrid.ca/>) and Compute Canada ([www.computecanada.ca](http://www.computecanada.ca)).

## References

- Achille, A. and Soatto, S. Information dropout: Learning optimal representations through noisy computation. *IEEE Transactions on Pattern Analysis and Machine Intelligence*, 40(12):2897–2905, 2018.
- Agarwal, A., Kakade, S. M., Lee, J. D., and Mahajan, G. Optimality and approximation with policy gradient methods in Markov decision processes. In Abernethy, J. and Agarwal, S. (eds.), *Proceedings of Thirty Third Conference on Learning Theory*, volume 125 of *Proceedings of Machine Learning Research*, pp. 64–66. PMLR, 2020.
- Andrychowicz, O. A. M., Baker, B., Chociej, M., Józefowicz, R., McGrew, B., Pachocki, J., Petron, A., Plappert, M., Powell, G., Ray, A., Schneider, J., Sidor, S., Tobin, J., Welinder, P., Weng, L., and Zaremba, W. Learning dexterous in-hand manipulation. *International Journal of Robotics Research*, 39(1):3–20, 2020.
- Arora, S., Choudhury, S., and Scherer, S. Hindsight is only 50/50: Unsuitability of mdp based approximate pomdp solvers for multi-resolution information gathering. *arXiv preprint arXiv:1804.02573*, 2018.
- Bertsekas, D. P. Approximate policy iteration: A survey and some new methods. *Journal of Control Theory and Applications*, 9(3):310–335, 2011.
- Bertsekas, D. P. *Reinforcement learning and optimal control*. Athena Scientific Belmont, MA, 2019.
- Bertsekas, D. P. and Tsitsiklis, J. N. An analysis of stochastic shortest path problems. *Mathematics of Operations Research*, 16(3):580–595, 1991.
- Biewald, L. Experiment Tracking with Weights and Biases, 2020. Software available from wandb.com.
- Chen, D., Zhou, B., Koltun, V., and Krähenbühl, P. Learning by cheating. In *Conference on Robot Learning*, pp. 66–75. PMLR, 2020.
- Chevalier-Boisvert, M., Willems, L., and Pal, S. Minimalistic gridworld environment for OpenAI gym. <https://github.com/maximecb/gym-minigrid>, 2018.
- Choudhury, S., Bhardwaj, M., Arora, S., Kapoor, A., Ranade, G., Scherer, S., and Dey, D. Data-driven planning via imitation learning. *The International Journal of Robotics Research*, 37(13-14):1632–1672, 2018.
- Deisenroth, M. P., Neumann, G., Peters, J., et al. A survey on policy search for robotics. *Foundations and trends in Robotics*, 2(1-2):388–403, 2013.
- Doshi-Velez, F., Pfau, D., Wood, F., and Roy, N. Bayesian nonparametric methods for partially-observable reinforcement learning. *IEEE transactions on pattern analysis and machine intelligence*, 37(2):394–407, 2013.
- Dosovitskiy, A., Ros, G., Codevilla, F., Lopez, A., and Koltun, V. CARLA: An open urban driving simulator. In *Proceedings of the 1st Annual Conference on Robot Learning*, pp. 1–16, 2017.
- Engstrom, L., Ilyas, A., Santurkar, S., Tsipras, D., Janoos, F., Rudolph, L., and Madry, A. Implementation matters in deep rl: A case study on ppo and trpo. In *International Conference on Learning Representations*, 2020.
- Finn, C., Tan, X. Y., Duan, Y., Darrell, T., Levine, S., and Abbeel, P. Deep spatial autoencoders for visuomotor learning. *Proceedings - IEEE International Conference on Robotics and Automation*, 2016-June:512–519, 2016.
- Igl, M., Zintgraf, L., Le, T. A., Wood, F., and Whiteson, S. Deep variational reinforcement learning for POMDPs. In *Proceedings of the 35th International Conference on Machine Learning*, volume 80 of *Proceedings of Machine Learning Research*, pp. 2117–2126. PMLR, 2018.
- Kaelbling, L. P., Littman, M. L., and Cassandra, A. R. Planning and acting in partially observable stochastic domains. *Artificial intelligence*, 101(1-2):99–134, 1998.
- Kamienny, P.-A., Arulkumaran, K., Behbahani, F., Boehmer, W., and Whiteson, S. Privileged information dropout in reinforcement learning. *arXiv preprint arXiv:2005.09220*, 2020.

- Kang, B., Jie, Z., and Feng, J. Policy optimization with demonstrations. In *Proceedings of the 35th International Conference on Machine Learning*, volume 80 of *Proceedings of Machine Learning Research*, pp. 2469–2478. PMLR, 2018.
- Kato, S., Takeuchi, E., Ishiguro, Y., Ninomiya, Y., Takeda, K., and Hamada, T. An Open Approach to Autonomous Vehicles. *IEEE Micro*, 35(6):60–68, 2015.
- Kingma, D. P. and Ba, J. Adam: A method for stochastic optimization. *arXiv preprint arXiv:1412.6980*, 2014.
- Könönen, V. Asymmetric multiagent reinforcement learning. *Web Intelligence and Agent Systems: An international journal*, 2(2):105–121, 2004.
- Lambert, J., Sener, O., and Savarese, S. Deep learning under privileged information using heteroscedastic dropout. In *Proceedings of the IEEE Conference on Computer Vision and Pattern Recognition*, pp. 8886–8895, 2018.
- Laskey, M., Lee, J., Fox, R., Dragan, A., and Goldberg, K. Dart: Noise injection for robust imitation learning. *arXiv preprint arXiv:1703.09327*, 2017.
- Laskin, M., Lee, K., Stooke, A., Pinto, L., Abbeel, P., and Srinivas, A. Reinforcement learning with augmented data. *arXiv preprint arXiv:2004.14990*, 2020.
- Laskin, M., Srinivas, A., and Abbeel, P. Curl: Contrastive unsupervised representations for reinforcement learning. *Proceedings of the 37th International Conference on Machine Learning, Vienna, Austria, PMLR 119*, 2020. [arXiv:2004.04136](https://arxiv.org/abs/2004.04136).
- Levine, S., Finn, C., Darrell, T., and Abbeel, P. End-to-end training of deep visuomotor policies. *Journal of Machine Learning Research*, 17:1–40, 2016.
- Littman, M. L., Cassandra, A. R., and Kaelbling, L. P. Learning policies for partially observable environments: Scaling up. *Seventh International Conference on Machine Learning*, pp. 362–370, 1995.
- Meng, Z., Li, J., Zhao, Y., and Gong, Y. Conditional teacher-student learning. In *ICASSP 2019-2019 IEEE International Conference on Acoustics, Speech and Signal Processing (ICASSP)*, pp. 6445–6449. IEEE, 2019.
- Murphy, K. P. A survey of POMDP solution techniques. *environment*, 2:X3, 2000.
- Nguyen, H., Daley, B., Song, X., Amato, C., and Platt, R. Belief-grounded networks for accelerated robot learning under partial observability. *arXiv preprint arXiv:2010.09170*, 2020.
- Pinto, L., Andrychowicz, M., Welinder, P., Zaremba, W., and Abbeel, P. Asymmetric actor critic for image-based robot learning. *arXiv preprint arXiv:1710.06542*, 2017.
- Rainforth, T., Cornish, R., Yang, H., Warrington, A., and Wood, F. On nesting Monte Carlo estimators. In *International Conference on Machine Learning*, pp. 4267–4276. PMLR, 2018.
- Ross, S. and Bagnell, J. A. Reinforcement and imitation learning via interactive no-regret learning. *arXiv preprint arXiv:1406.5979*, 2014.
- Ross, S., Gordon, G. J., and Bagnell, J. A. A reduction of imitation learning and structured prediction to no-regret online learning. *Journal of Machine Learning Research*, 15:627–635, 2011.
- Salter, S., Rao, D., Wulfmeier, M., Hadsell, R., and Posner, I. Attention-privileged reinforcement learning. *arXiv preprint arXiv:1911.08363*, 2019.
- Sasaki, F. and Yamashina, R. Behavioral cloning from noisy demonstrations. In *International Conference on Learning Representations*, 2021.
- Schulman, J., Levine, S., Abbeel, P., Jordan, M., and Moritz, P. Trust region policy optimization. In *International conference on machine learning*, pp. 1889–1897, 2015.
- Schulman, J., Moritz, P., Levine, S., Jordan, M., and Abbeel, P. High-dimensional continuous control using generalized advantage estimation. *arXiv preprint arXiv:1506.02438*, 2015.
- Schulman, J., Wolski, F., Dhariwal, P., Radford, A., and Klimov, O. Proximal policy optimization algorithms. *arXiv preprint arXiv:1707.06347*, 2017.
- Schwab, D., Springenberg, J. T., Martins, M. F., Neunert, M., Lampe, T., Abdolmaleki, A., Hertweck, T., Hafner, R., Nori, F., and Riedmiller, M. A. Simultaneously learning vision and feature-based control policies for real-world ball-in-a-cup. In *Robotics: Science and Systems XV*, 2019.
- Song, J., Lanka, R., Yue, Y., and Ono, M. Co-training for policy learning. *35th Conference on Uncertainty in Artificial Intelligence*, 2019.
- Spaan, M. T. J. *Partially Observable Markov Decision Processes*, pp. 387–414. Springer Berlin Heidelberg, 2012. ISBN 978-3-642-27645-3.
- Sun, W., Venkatraman, A., Gordon, G. J., Boots, B., and Bagnell, J. A. Deeply AggreVaTeD: Differentiable imitation learning for sequential prediction. In Precup, D. and Teh, Y. W. (eds.), *Proceedings of the 34th International Conference on Machine Learning*, volume 70 of *Proceedings of Machine Learning Research*, pp. 3309–3318. PMLR, 2017.

- Sun, W., Bagnell, J. A., and Boots, B. Truncated horizon policy search: Combining reinforcement learning & imitation learning. *6th International Conference on Learning Representations*, pp. 1–14, 2018.
- Sutton, R. *Reinforcement Learning*. The Springer International Series in Engineering and Computer Science. Springer US, 1992. ISBN 9780792392347.
- Vapnik, V. and Vashist, A. A new learning paradigm: Learning using privileged information. *Neural networks*, 22 (5-6):544–557, 2009.
- Weihs, L., Jain, U., Salvador, J., Lazebnik, S., Kembhavi, A., and Schwing, A. Bridging the imitation gap by adaptive insubordination. *arXiv preprint arXiv:2007.12173*, 2020.
- Williams, R. J. Simple statistical gradient-following algorithms for connectionist reinforcement learning. *Machine learning*, 8(3-4):229–256, 1992.
- Wymann, B., Espie, C. G., Dimitrakakis, C., Coulom, R., and Sumner, A. TORCS: The Open Racing Car Simulator, 2014.
- Yarats, D., Kostrikov, I., and Fergus, R. Image augmentation is all you need: Regularizing deep reinforcement learning from pixels. In *International Conference on Learning Representations*, 2021.

## A. Table of Notation

Symbol	Name	Alternative Name(s)	Type	Description
$t$	Time	Discrete time step	$\mathbb{Z}$	Discrete time step used in integration. Indexes other values.
$s_t$	State	Full state, compact state, omniscient state	$\mathcal{S} = \mathbb{R}^D$	State space of the MDP. Sufficient to fully define state of the environment.
$o_t$	Observation	Partial observation	$\mathcal{O} = \mathbb{R}^{A \times B \times \dots}$	Observed value in POMDP, emitted conditional on state. State is generally not identifiable from observation. Conditionally dependent only on state.
$a_t$	Action		$\mathcal{A} = \mathbb{R}^K$	Interaction made with the environment at time $t$ .
$r_t$	Reward		$\mathcal{R}$	Value received at time $t$ indicating performance. Maximising sum of rewards is the objective.
$b_t$	Belief state		$\mathcal{B}$	
$q_\pi$	Trajectory distribution		$\mathcal{Q} : \Pi \rightarrow (\mathcal{A} \times \mathcal{B} \times \mathcal{O} \times \mathcal{S}^2 \times \mathcal{R})^{t+1}$	Process of sampling trajectories using the policy $\pi$ . If the process is fully observed $\mathcal{O} = \emptyset$ .
$\tau_{0:t}$	Trajectory	Rollouts	$(\mathcal{A} \times \mathcal{B} \times \mathcal{O} \times \mathcal{S}^2 \times \mathcal{R})^{t+1}$	Sequence of tuples containing state, next state, observation, action and reward.
$\gamma$	Discount factor		$\Gamma = [0, 1]$	Factor attenuating future reward in favor of near reward.
$p(s_{t+1}   s_t, a_t)$	Transition distribution	Plant model, environment	$\mathcal{T} : \mathcal{S} \times \mathcal{A} \rightarrow \mathcal{S}$	Defines how state evolves, conditional on the previous state and the action taken.
$p(o_t   s_t)$	Emission distribution	Observation function	$\mathcal{Y} : \mathcal{S} \rightarrow \mathcal{O}$	Distribution over observed values conditioned on state.
$p(s_0)$	Initial state distribution	State prior	$\mathcal{T}_0 : \rightarrow \mathcal{S}$	Distribution over state at $t = 0$ .
$\pi_\theta(a_t   s_t)$	MDP policy	Expert, omniscient policy, asymmetric expert, asymmetric policy	$\Pi_\Theta : \mathcal{S} \rightarrow \mathcal{A}$	Distribution over actions conditioned on state. Only used in MDP.
$\theta$	MDP policy parameters		$\Theta$	Parameters of MDP policy. Cumulative reward is maximized over these parameters.
$\pi_\phi(a_t   b_t)$	POMDP policy	Agent, partially observing policy	$\Pi_\Phi : \mathcal{B} \rightarrow \mathcal{A}$	Distribution over actions conditioned on belief state. Only used in POMDP.
$\phi$	POMDP policy parameters		$\Phi$	Parameters of MDP policy. Cumulative reward is maximized over these parameters.
$\pi_\psi(a_t   b_t)$	Variational trainee policy	Variational approximation	$\Pi_\Psi : \mathcal{B} \rightarrow \mathcal{A}$	Variational approximation of the implicit policy.
$\psi$	Variational trainee policy parameters		$\Psi$	Parameters of the variational approximation of the implicit policy.
$\pi_\beta$	Mixture policy		$\Pi_\beta : \mathcal{S} \times \mathcal{B} \rightarrow \mathcal{A}$	Mixture of MDP policy ( $\pi_\theta$ ) and POMDP policy ( $\pi_\phi$ ).
$\beta$	Mixing coefficient		$[0, 1]$	Fraction of MDP policy used in mixture policy.
$D$	Replay buffer	Data buffer	$\mathcal{D} = \{\tau_0 : \tau_n\}_{n \in 1:N}$	Store to access previous trajectories. Facilitates data re-use.
$\mathbb{KL}[p  q]$	Kullback–Leibler divergence	KL divergence, forward KL, mass-covering KL		Particular divergence between two distributions. Forward KL is mass covering. Reverse KL ( $\mathbb{KL}[q  p]$ ) is mode seeking.
$Q^\pi(s_t, a_t)$	Q-function	State Q-function	$\mathcal{Q}_s : \mathcal{S} \times \mathcal{A} \rightarrow \mathbb{R}$	Expected sum of rewards ahead, garnered by taking action $a_t$ in state $s_t$ induced by policy $\pi$ .
$Q^\pi(b_t, a_t)$	Belief state Q-function		$\mathcal{Q}_b : \mathcal{B} \times \mathcal{A} \rightarrow \mathbb{R}$	Expected sum of rewards ahead, garnered by taking action $a_t$ in belief state $b_t$ induced by policy $\pi$ .
$\hat{\pi}_\theta(a_t   b_t)$	Implicit policy		$\Pi_\Phi : \mathcal{B} \rightarrow \mathcal{A}$	Agent policy obtained by marginalizing over state given belief state. Closest approximation of $\pi_\theta$ under partial observability. Approximated by $\pi_\phi$ .
$d^\pi(s_t, b_t)$	Occupancy	Discounted state visitation distribution (Agarwal et al., 2020)	$M : \mathcal{S} \times \mathcal{B} \rightarrow \mathbb{R}$	Joint density of $s_t = s$ and $b_t = b$ given policy $\pi$ . Marginal of $q_\pi$ over previous and future states, belief states, and all actions, observations and rewards.
$\pi_\eta$	Fixed reference distribution		$\Pi$	Fixed distribution that is rolled out under to generate samples that are used in gradient calculation.

Table A.1: Notation and definitions used throughout the main paper.

## B. Additional Experimental Results

### B.1. Alternative Policy Gradient Algorithms

We highlighted in Section 5 that A2D can be used with any REINFORCE-based policy gradient algorithm. We demonstrate this by using PPO (Schulman et al., 2017) as the policy gradient update ( $\text{RLStep}$  in Algorithm 1) in A2D, instead of TRPO, and comparing the performance of these variants to direct application of RL. All experiments use the high-dimensional, partial, image-based inputs. The results for this experiment are shown in Figure B.1. We see that PPO actually diverges for image-based inputs, and, as in Figure 4, direct application of TRPO is slow. In contrast, A2D converges to the optimal solution, with a convergence rate that is very similar for PPO and TRPO. This highlights how A2D is largely agnostic to the policy gradient method used to update the expert policy. We believe that performing RL in the low-dimensional, omniscient state representation simplifies the RL task to the point where the results are less sensitive to the specifics of the RL algorithm. Furthermore, this shifts much of the perception complexity to the low-variance and easy-to-tune IL component. As such, we do not suggest that A2D is a “better RL algorithm,” but is instead a way of formulating and tackling a problem such that the favorable properties of asymmetric imitation learning operating on POMDPs, and RL operating on MDPs, are both retained. To perform this experiment we only needed to substitute a single line of code switching which gradient update was used.

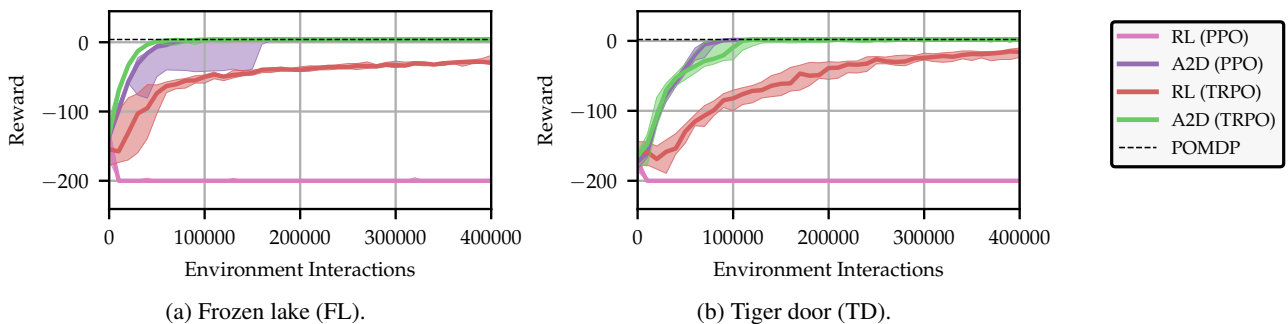


Figure B.1: Results for using PPO (Schulman et al., 2017) compared with TRPO (Schulman et al., 2017). We see that PPO diverges for image-based representations (pink). However, when used in A2D with image-based representations (purple), the correct solution is recovered. Furthermore, this solution is recovered in a similar number of environment interactions compared to TRPO, and only lags slightly behind the performance of the best-case MDP. This shows that A2D can be used, with minimal modifications, with a range of policy-gradient based RL algorithms. We use a learning rate of  $7e-3$  for learning all function approximators, a batch and buffer size of 2,000 samples, an entropy regularizer of 0.001 applied to the surrogate loss, and decayed  $\beta$  at a rate of 0.8. We show the median and quartiles across ten random seeds.

## B.2. Differences in Representation

In Figure B.2 we investigate the trainee using different representations in A2D. Specifically, we investigate using a compact-but-partial vector representation (labeled as *Compact*), and the original image-based representation. Both representations include the same partial information, but the compact representation is a much more efficient representation for RL. The compact representation for frozen lake is a length 25 one-hot vector representing the position of the agent. For tiger door the compact representation is the concatenation of three one-vectors: a length 25 one-hot vector encoding the position of the agent, a length two vector encoding the position of the goal, and a length two vector encoding the position of the hazard. The goal and hazard vectors are all zeros until the button is pressed, at which time they become one-hot vectors. This can be considered as the optimal encoding of the observation and action history. We note that analytically recovering such an encoding is not always possible (in the AV example, for instance), and learning an encoding (c.f. *Pre-Enc* in Figure 4) is unreliable, introduces a non-trivial amount of additional complexity and hyperparameter tuning.

Results are shown in Figure B.2. We see performing RL directly on the compact representation (orange) is fast and stable. Direct RL in the image-based representation (red) is slow, and does not converge within the computational budget. We see for both ice lake and tiger door A2D converges in a similar number of interactions, and, that this convergence rate is commensurate with the convergence of an omniscient expert. This shows that A2D has successfully abstracted the perception task into the efficient AIL step, and performs RL in the efficient and low-variance omniscient state representation. This means that A2D is able to exploit the relative strengths of RL to offset the weaknesses of AIL, and vice versa, in an efficient, low-overhead and end-to-end manner. Crucially, the expert is co-trained with the agent/trainee, and hence there is no requirement for pre-specified expert policies or example trajectories from which to learn policies or static encoders.

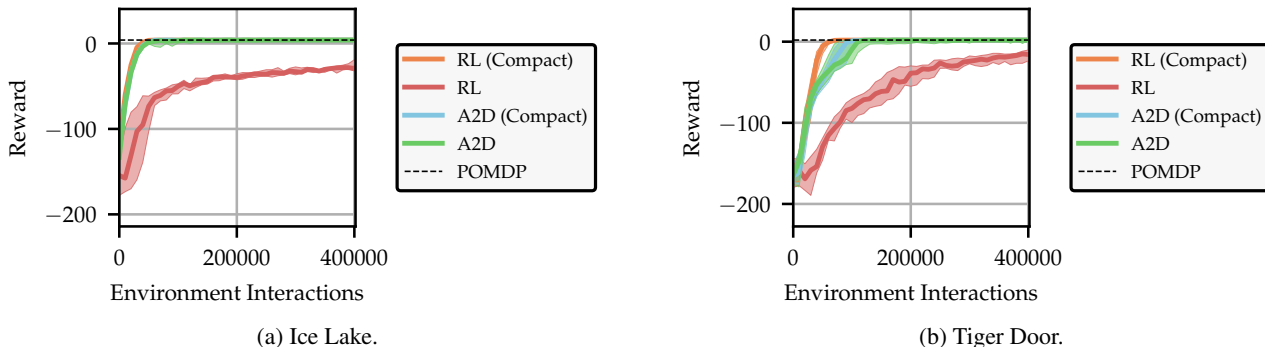


Figure B.2: Training curves comparing convergence of A2D and vanilla RL on the POMDP for compact (one-hot vector) representations and image-based representations. We see that the RL converges quickly on the compact representation (orange) and slowly for images (red). A2D on the other hand converges in a sample complexity commensurate with operating directly on the compact MDP for *both* image-based and compact representations. This confirms our hypothesis that A2D can reduce the complexity of operating in high-dimensional, partially observed environments to a complexity commensurate with the best-possible convergence rate obtained by performing RL directly on the most efficient encoding or complete state.

### B.3. Convergence of Reward and Divergence

In Figure B.3 we show the convergence of the expert and trainee (partially observing agent learned through AIL), alongside the evolution of the divergence between the expert policy and trainee policy. We see that the  $\mathbb{KL}$  divergence rises initially, as the expert is optimizing for the MDP while  $\beta$  is close to one. Then, as  $\beta$  approaches zero, the divergence falls as the expert is forced to optimize the Q function of the trainee. This is particularly highlighted in B.3b where the expert learns to *not* go directly to the goal, and should instead push the button. Annealing  $\beta$  more slowly emphasizes this behavior.

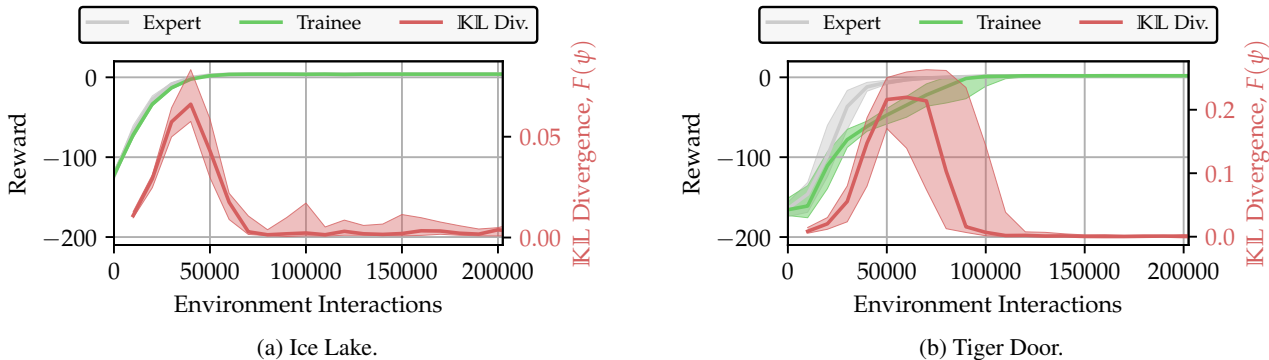


Figure B.3: Additional results for the gridworld experiments presented in Figure 4. Training curves for the expert and trainee during A2D training, and the projection loss between the expert and trainee. Due to the annealing effect of  $\beta$  we can see that the  $\mathbb{KL}$  divergence between expert and trainee (projection loss) rises as the expert learns to solve the MDP, but then reduces to zero as  $\beta$  approaches zero and the POMDP is solved instead. This is particularly pronounced in tiger door, where the performance of the trainee lags behind slightly, as the expert actually optimizes the MDP, initially limiting the performance in the POMDP, before being forced to optimize the POMDP, and then closing the performance gap. Both expert and trainee converge to the same reward and form an identifiable process pair.

#### B.4. Estimating the Q function

In Section 5 we briefly discussed the possibility of not explicitly estimating the Q function. All the terms in Equation (24) can be computed directly with the exception of the Q function. One approach therefore is to train an additional function approximator targeting the Q function directly. This can then be used to estimate the discounted sum of rewards ahead given a particular action and state without directly using the Monte Carlo rollouts. However, estimating the Q function increases the computational cost, increases the number of hyperparameters that need tuning, and can lead to instabilities and biased training by overly relying on imperfect function approximators. Therefore, as in many on-policy RL algorithms, an alternative is to use Monte Carlo estimates of the Q function, computed directly from a sampled trajectory (c.f. Equation (25)-(27)).

However, somewhat unexpectedly, this second approach can lead to the systemic failure of A2D in particular *environments*. This can be shown by expanding the definition of  $Q^{\pi_\psi}(a, b)$ , as per Equation (19):

$$Q^{\pi_\psi}(a, b) = \mathbb{E}_{p(s'|a,b)} \left[ d^{\pi_\psi}(b'|s') \left[ r(s, a, s') + \gamma \mathbb{E}_{\pi_\psi(a'|b')} [Q^{\pi_\psi}(a', b')] \right] \right], \quad (\text{B.1})$$

where  $s'$  is the state after taking action  $a$  in belief state  $b$ . Since sampling from  $d^{\pi_\psi}(b'|s')$  is intractable, directly using the trajectories is equivalent to using a single trajectory throughout this expression. Using single-sample estimates of the outer expectation in Equation (B.1), where the belief state used is the same as in the gradient evaluation in Equation (25), can bias the estimator by re-using random variables within nested expectations (Rainforth et al., 2018). This therefore biases the gradient estimator as the gradient is *not* conditionally independent of the current (unobserved) state given the belief state. This in turn introduces a correlation that essentially allows the expert to “cheat” by learning using exclusively the true state for a *single* time step of a trajectory.

When the Q function is estimated directly, the outer marginalization in Equation (B.1) is estimated directly, and hence the learned Q function amortizes this expectation by learning across many different sampled trajectories. Therefore, from the theoretical perspective, estimating the Q function is important for A2D to be guaranteed to function. However, we find that this bias is only exhibited in very specific environments, and hence, in most environments, the Q function does not need to be estimated. This reduces the computational cost of the algorithm, reduces the number of hyperparameters and network architectures that need tuning, reduces the dependence on function approximators, and, as we show in Figure B.4, can accelerate convergence in suitable environments.

We explore this behavior empirically in Figure B.4 and B.5. We introduce three variants of the tiger door problem. The first variant, tiger door 1, shown in Figure B.4a, actually corresponds to the original tiger door problem (Littman et al., 1995). Tiger door 2 and 3, shown in Figures B.4b and B.4c, then separate the goal by one and two squares respectively. The analysis above predicts that tiger door 1 should not be solvable without direct estimation of the Q function, as reaching the goal directly ends the episode, and hence the marginalization in Equation (B.1) cannot naturally occur within the trajectory. This forces the expert to put more mass on directly proceeding to the goal, even though the goal is not visible. However, in tiger door 2 and 3, the episode does not immediately end after proceeding directly towards the goal, and hence provides an unbiased, single sample estimate of the marginal, and no Q function is required.

The predicted behavior is indeed observed when applying A2D to each environment with and without a Q function, as shown in Figure B.4. We see that with the Q function, the correct policy is always recovered. However, in tiger door 2 and 3, the correct policy is recovered more slowly when the Q function is being learned. This is likely due to the slight bias introduced by using an imperfect Q function. However, in tiger door 1 when the Q function is not estimated the incorrect behavior is recovered as predicted, with the agent forced into heading directly to one of the potential goal positions without pushing the button, and receiving a low reward.

We also include demonstration of this in Figure B.5, instead showing the evolution of the expert and agent/trainee during training, across the three tiger doors, with and without an explicit Q function. Again, we see that learning the Q function learns the correct behavior in all scenarios. We see again that the  $\mathbb{KL}$  divergence first rises, as  $\beta$  is closer to one, and hence the expert is optimizing the MDP, before falling to zero as  $\beta \rightarrow 0$ . It is highlighted in Figure B.5b that using Q leads to more variable optimization paths and slower convergence. However, we note that the divergence between the expert and trainee is always lower when Q is learned directly, suggesting that learning Q forces the expert to more faithfully optimize the reward of the agent, albeit at the cost of in turn subtly biasing the agent.

We therefore initially suggest that the Q function is not estimated, and the advantage is estimated directly from the Monte



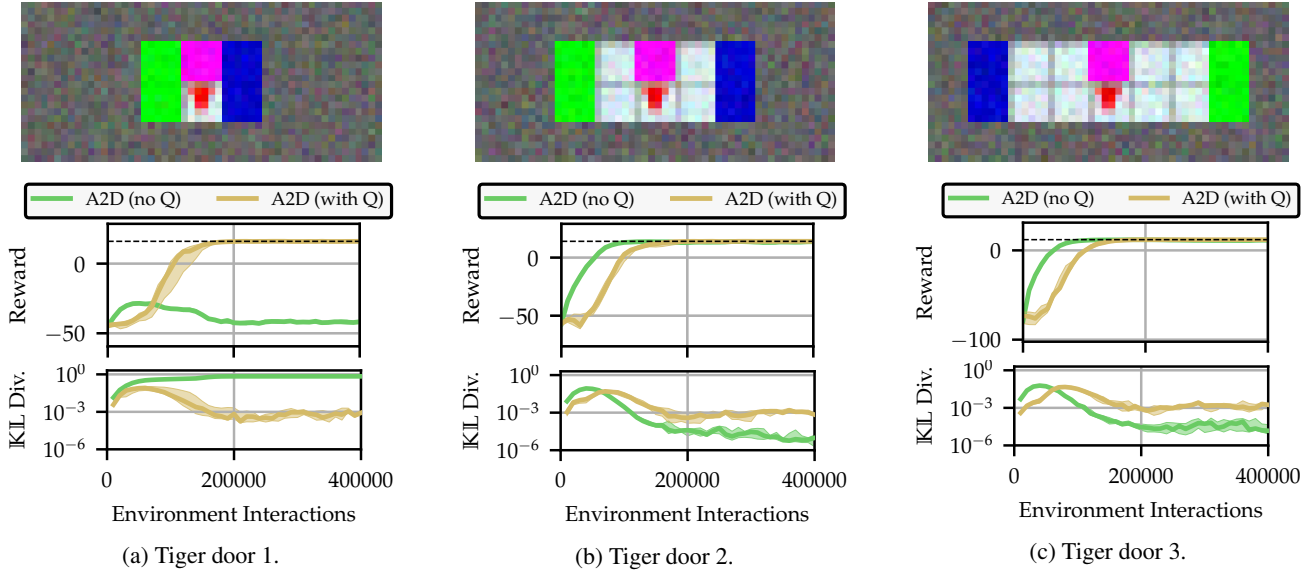


Figure B.4: Results investigating requirement of directly estimating the Q function, as initially introduced in Section 5 and discussed further in Section B.4. Mean and quartiles across ten random seeds are shown. The Q function is learned targeting the expected discounted sum of rewards ahead conditioned on a particular action. A value function is then learned, and used in conjunction with the Q function to directly estimate the advantage in Equation (25). Hence the A2D gradient is computed without direct use of Monte Carlo rollouts. When no Q function is being used, the advantage is computed using GAE (c.f. Equations (25)-(27)). Figure B.4a: Training curves for the original tiger door problem (Littman et al., 1995). As predicted by the discussion in Section B.4, A2D does not converge to the correct policy if a Q function is not simultaneously learned. This deficiency is instrumented by the high  $\mathbb{KL}$  divergence during training. If a Q function is learned the desired partially observed behavior is recovered and there is a low divergence between policies. Figure B.4b and B.4c: By separating the goal by at least one square means desired behavior is recovered regardless of whether a Q function is used. This is because an unbiased single-sample estimate of the marginalization in Equation (B.1) is recovered due to the introduction of additional random variables. However, convergence is slower when using a Q function, and, is somewhat more variable (more strongly indicated in Figure B.5).

Carlo trajectories. There are then two instruments available to diagnose if a Q function must be directly approximated: if there is consistently a performance gap between the expert policy and the agent policy, or, if there is a non-negligible  $\mathbb{KL}$  divergence between the expert and agent policy (indicating the policies are not being forced to be identifiable). If either of these behaviors are observed, then a Q function should be directly estimated. While the discussion and example presented in this example provide some explanation of this behavior, we were unable to provide a concrete definition or condition describing when estimating a Q function is required. This behavior is a function of the *environment*, and hence there may be no readily available or easy-to-test condition for when a Q function is required. This behavior may manifest as a complication in any method for ameliorating the drawbacks of AIL, and hence further investigating this is a challenging, interesting, and potentially pivotal topic for future research.

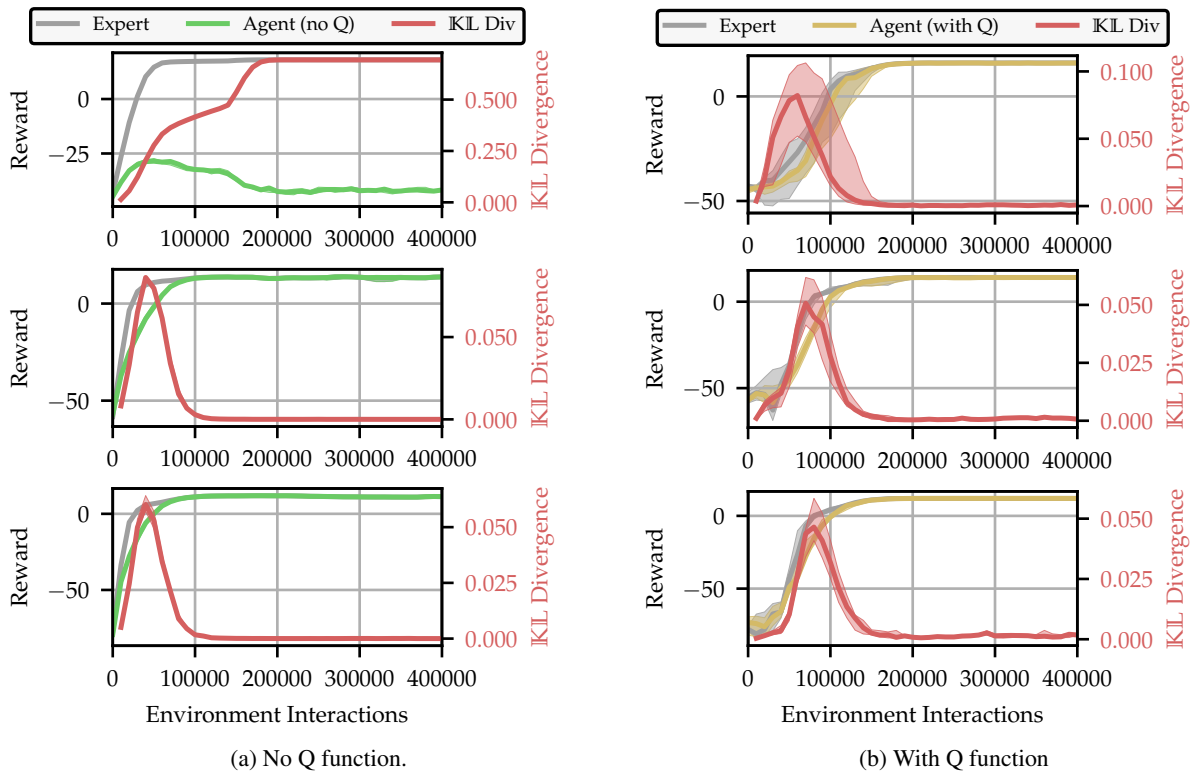


Figure B.5: Results showing the performance of A2D during training when exploring explicitly whether to directly estimate the Q function. The top, middle and bottom rows correspond to tiger door 1, 2 and 3 respectively. In tiger door 1, when a Q function is not used, the expert and agent/trainee do not converge to the same solution, as indicated by the high divergence loss in the top left figure. However, when a Q function is used, convergence is slower, and, the optimization path is more variable, suggesting that there is increased bias/variance in the gradient estimator. This instability may be critical when tackling more complex problems with larger action spaces. This leads us to propose that the “default” A2D algorithm does not directly estimate the Q function. If the desired behavior is not being recovered (instrumented by a non-zero  $\mathbb{K}\mathbb{L}$  divergence), then a Q function should be estimated. The median and quartiles across ten random seeds are shown.

## C. Additional Proofs

In this section we provide full proofs for the material presented in the main text. These proofs describe more completely how the A2D estimator is constructed. We briefly give an overview of how the following proofs and details are laid out.

We begin in Section C.1 by discussing in more detail the occupancy  $d^\pi(s, b)$ . This joint occupancy is a convenient term to define as it allows us to compactly denote the probability that an agent is in a particular state and belief state at any point in time. We can then construct conditional and marginal occupancies by operating on this joint occupancy.

In Section C.2 we analyze the behavior of AIL. We first detail a full proof of Theorem 1, stating that the implicit policy is the solution to the minimization of the most conveniently defined AIL objective, where the trainee simply imitates the expert at each state-belief state pair. This allows us to compactly write and analyze the solution to AIL as the implicit policy. However, the implicit policy is defined by an intractable inference over the conditional occupancy,  $d^\pi(s|b)$ , from which we cannot sample.

We therefore show in Section C.2.2 that we can define a variational approximation to the implicit policy, referred to as a *trainee*, that is learned using the AIL objective. We construct an estimator of the gradient of the trainee parameters to learn this trainee, under a fixed distribution over trajectories, directly targeting the result of the inference defined by the implicit policy. Crucially, the trainee can be learned using samples from the joint occupancy,  $d^\pi(s, b)$ , from which we *can* sample (instead of samples from the conditional  $d^\pi(s|b)$  as per the implicit policy). If the variational family is sufficiently expressive, this minimization can be performed exactly.

We then show that an iterative AIL approach, that updates the fixed distribution over trajectories at each iteration, recovers the desired trainee. We then show that the limiting behavior of this iterative algorithm is equivalent to learning under the occupancy of the implicit policy. Finally, using these results, we then prove Theorem 2, which shows that for an identifiable MDP-POMDP pair, the iterative AIL approach outlined above recovers an optimal partially observing policy.

However, identifiability is a *very* strong condition. Therefore, mitigating unidentifiability in AIL is primary the motivation behind A2D. In Section C.3 we provide a proof of the “exact” form of A2D. We begin by providing additional detail on intermediate results, including a brief explanation of the policy bound stated in Equations (21)-(22), a derivation of the Q-based A2D update in Equation (24), and the advantage-based update in Equation (25). We then use the assumptions, intermediate lemmas, and theorems to prove exact A2D (using a similar strategy as we used to prove Theorem 2). This verifies that, under exact updates, A2D converges to the optimal partially observing policy. We then conclude by evaluating the requirements of this algorithm.

### C.1. Occupancy Measures

Throughout this paper we use  $q_\pi(\tau)$  as general notation for the trajectory generation process, indicating which policy is used to generate the trajectory as a subscript (c.f. Equation (1) and Equation (5)). We define  $d^\pi(s, b)$ , referred to as the *joint occupancy*, as the time-marginal of  $q_\pi(\tau)$  over all variables in the trajectory other than  $s$  and  $b$ :

$$d^\pi(s, b) = (1 - \gamma) \int_{\tau \in \mathcal{T}} \sum_{t=0}^{\infty} \gamma^t q_\pi(\tau) \delta(s_t - s) \delta(b_t - b) d\tau, \quad \text{where } \gamma \in [0, 1), \quad (\text{C.1})$$

$$d^\pi(s) = \int_{b' \in \mathcal{B}} d^\pi(s, b') db', \quad d^\pi(s|b) = \int_{b' \in \mathcal{B}} d^\pi(s, b') \delta(b' - b) db', \quad (\text{C.2})$$

$$d^\pi(b) = \int_{s' \in \mathcal{S}} d^\pi(s', b) ds', \quad d^\pi(b|s) = \int_{s' \in \mathcal{S}} d^\pi(s', b) \delta(s' - s) ds'. \quad (\text{C.3})$$

We refer the reader to §3 of Agarwal et al. (2020) for more discussion on the occupancy (described instead as a *discounted state visitation distribution*). Despite the complex form of these expressions, we can sample from the joint occupancy  $d^\pi(s, b)$  by simply rolling out under the policy  $\pi$  according to  $q_\pi(\tau)$ , and taking a random state-belief state pair from the trajectory. We can then trivially obtain a sample from either marginal occupancy,  $d^\pi(s)$  or  $d^\pi(b)$ , by simply dropping the other variable. We can also recover a *single* sample, for a *sampled*  $b$ , from the conditional occupancy  $d^\pi(s|b)$  by taking the associated  $s$  (and vice-versa for conditioning on a sampled  $s$ ). However, and critically for this work, sampling multiple states or belief states from either conditional occupancy is intractable. Therefore, much of the technical work presented is carefully constructing and manipulating the learning task such that we can use samples from the joint occupancy (from which we can sample), in-place of samples from the conditional occupancy (from which we cannot sample).

## C.2. Analysis of AIL

We begin by analyzing the behavior of AIL. This will allow us to subsequently define the behavior of A2D by building on these results.

### C.2.1. PROOF OF THEOREM 1

We first verify the claim that the implicit policy minimizes the AIL objective.

**Theorem 1** (Asymmetric IL Target, reproduced from Section 3). *For any fully observing policy  $\pi_\theta \in \Pi_\Theta$  and fixed policy  $\pi_\eta$ , the implicit policy  $\hat{\pi}_\theta^\eta \in \hat{\Pi}_\Theta$ , defined in Definition 1, minimizes the following asymmetric IL objective:*

$$\hat{\pi}_\theta^\eta(a|b) = \arg \min_{\pi \in \Pi} \mathbb{E}_{d^{\pi_\eta}(s,b)} [\mathbb{KL}[\pi_\theta(a|s) \parallel \pi(a|b)]] . \quad (\text{C.4})$$

*Proof.* Considering first the optima of the right-hand side:

$$\pi^*(a|b) = \arg \min_{\pi \in \Pi} \mathbb{E}_{d^{\pi_\eta}(s,b)} [\mathbb{KL}[\pi_\theta(a|s) \parallel \pi(a|b)]] , \quad (\text{C.5})$$

and expanding the expectation and  $\mathbb{KL}$  term:

$$\pi^*(a|b) = \arg \min_{\pi \in \Pi} \mathbb{E}_{d^{\pi_\eta}(b)} \left[ \int_{s \in \mathcal{S}} \int_{a \in \mathcal{A}} \pi_\theta(a|s) \log \left( \frac{\pi_\theta(a|s)}{\pi(a|b)} \right) da d^{\pi_\theta}(s|b) ds \right] , \quad (\text{C.6})$$

$$= \arg \min_{\pi \in \Pi} \mathbb{E}_{d^{\pi_\eta}(b)} \left[ \int_{s \in \mathcal{S}} \int_{a \in \mathcal{A}} \pi_\theta(a|s) \log \pi_\theta(a|s) da d^{\pi_\eta}(s|b) ds \right] - \quad (\text{C.7})$$

$$\mathbb{E}_{d^{\pi_\eta}(b)} \left[ \int_{s \in \mathcal{S}} \int_{a \in \mathcal{A}} \pi_\theta(a|s) \log \pi(a|b) da d^{\pi_\eta}(s|b) ds \right] , \quad (\text{C.8})$$

$$= \arg \min_{\pi \in \Pi} K - \mathbb{E}_{d^{\pi_\eta}(b)} \left[ \int_{s \in \mathcal{S}} \int_{a \in \mathcal{A}} \pi_\theta(a|s) \log \pi(a|b) da d^{\pi_\eta}(s|b) ds \right] , \quad (\text{C.9})$$

where  $K$  is independent of  $\pi$ . Manipulating the rightmost term:

$$\pi^*(a|b) = \arg \min_{\pi \in \Pi} K - \mathbb{E}_{d^{\pi_\eta}(b)} \left[ \int_{a \in \mathcal{A}} \int_{s \in \mathcal{S}} \pi_\theta(a|s) d^{\pi_\eta}(s|b) ds \log \pi(a|b) da \right] , \quad (\text{C.10})$$

$$= \arg \min_{\pi \in \Pi} K - \mathbb{E}_{d^{\pi_\eta}(b)} \left[ \int_{a \in \mathcal{A}} \hat{\pi}_\theta^\eta(a|b) \log \pi(a|b) da \right] , \quad (\text{C.11})$$

We are now free to set the value of  $K$ , which we denote as  $K'$ , so long as it remains independent of  $\pi$  as this does not alter the minimizing argument:

$$K' = \mathbb{E}_{d^{\pi_\eta}(b)} \left[ \int_{a \in \mathcal{A}} \hat{\pi}_\theta^\eta(a|b) \log \hat{\pi}_\theta^\eta(a|b) da \right] , \quad (\text{C.12})$$

$$\pi^*(a|b) = \arg \min_{\pi \in \Pi} K' - \mathbb{E}_{d^{\pi_\eta}(b)} \left[ \int_{a \in \mathcal{A}} \hat{\pi}_\theta^\eta(a|b) \log \pi(a|b) da \right] , \quad (\text{C.13})$$

$$= \arg \min_{\pi \in \Pi} \mathbb{E}_{d^{\pi_\eta}(b)} \left[ \int_{a \in \mathcal{A}} \hat{\pi}_\theta^\eta(a|b) \log \hat{\pi}_\theta^\eta(a|b) da - \int_{a \in \mathcal{A}} \hat{\pi}_\theta^\eta(a|b) \log \pi(a|b) da \right] . \quad (\text{C.14})$$

Combining the logarithms:

$$\pi^*(a|b) = \arg \min_{\pi \in \Pi} \mathbb{E}_{d^{\pi_\eta}(b)} \left[ \int_{a \in \mathcal{A}} \hat{\pi}_\theta^\eta(a|b) \log \left( \frac{\hat{\pi}_\theta^\eta(a|b)}{\pi(a|b)} \right) da \right] , \quad (\text{C.15})$$

$$= \arg \min_{\pi \in \Pi} \mathbb{E}_{d^{\pi_\eta}(b)} [\mathbb{KL}[\hat{\pi}_\theta^\eta(a|b) \parallel \pi(a|b)]] . \quad (\text{C.16})$$

Assuming that the policy class  $\Pi$  is sufficiently expressive, this  $\mathbb{KL}$  can be exactly minimized, and hence we arrive at the desired result:

$$\pi^*(a|b) = \hat{\pi}_\theta^\eta(a|b), \quad \forall a \in \mathcal{A}, b \in \{b' \in \mathcal{B} \mid d^{\pi_\eta}(b') > 0\} . \quad (\text{C.17})$$

□

This proof shows that learning the trainee policy ( $\pi$  here,  $\pi_\psi$  later) using  $\mathbb{KL}$  minimization imitation learning (as in Equation (13)) recovers the policy defined as the implicit policy (as defined in Definition 1), and hence our definition of the implicit policy is well founded.

### C.2.2. VARIATIONAL IMPLICIT POLICY

However, the implicit policy is defined as an intractable inference problem, marginalizing over  $d^\pi(s|b)$ , from which we cannot sample. Therefore, we can further define a variational policy,  $\pi_\psi \in \Pi_\Psi$ , to approximate this policy, from which evaluating densities and sampling is more tractable. This policy can be learned using gradient descent:

**Lemma 1** (Variational Implicit Policy Update, c.f. Section 3, Equation (16)). *For an MDP  $\mathcal{M}_\Theta$ , POMDP  $\mathcal{M}_\Phi$ , and implicit policy  $\hat{\pi}_\theta$  (Definition 1), if we define a variational approximation to  $\hat{\pi}_\theta$ , parameterized by  $\psi$ , denoted  $\pi_\psi \in \Pi_\Psi$ , such that the following divergence is minimized:*

$$\psi^* = \arg \min_{\psi \in \Psi} F(\psi) = \arg \min_{\psi \in \Psi} \mathbb{E}_{d^{\hat{\pi}_\theta}(b)} [\mathbb{KL} [\hat{\pi}_\theta(a|b) || \pi_\psi(a|b)]], \quad (\text{C.18})$$

then an unbiased estimator for the gradient of this objective is given by the following expression:

$$\nabla_\psi F(\psi) = -\mathbb{E}_{d^{\hat{\pi}_\theta}(s,b)} [\mathbb{E}_{\pi_\theta(a|s)} [\nabla_\psi \log \pi_\psi(a|b)]] . \quad (\text{C.19})$$

*Proof.* Note the objective in Equation (C.18) is directly derived from the original AIL objective via Theorem 1. By manipulating the  $\mathbb{KL}$  term, pulling out terms that are constant with respect to  $\psi$ , and rearranging the expectations we obtain:

$$F(\psi) = \mathbb{E}_{d^{\hat{\pi}_\theta}(b)} [\mathbb{KL} [\hat{\pi}_\theta(a|b) || \pi_\psi(a|b)]], \quad (\text{C.20})$$

$$= \mathbb{E}_{d^{\hat{\pi}_\theta}(b)} \left[ \int_{a \in \mathcal{A}} \log \left( \frac{\hat{\pi}_\theta(a|b)}{\pi_\psi(a|b)} \right) \hat{\pi}_\theta(a|b) da \right], \quad (\text{C.21})$$

$$= \int_{b \in \mathcal{B}} \int_{a \in \mathcal{A}} -\log \pi_\psi(a|b) \hat{\pi}_\theta(a|b) da d^{\hat{\pi}_\theta}(b) db + C, \quad (\text{C.22})$$

$$= - \int_{b \in \mathcal{B}} \int_{a \in \mathcal{A}} \log \pi_\psi(a|b) \int_{s \in \mathcal{S}} \pi_\theta(a|s) d^{\hat{\pi}_\theta}(s|b) ds da d^{\hat{\pi}_\theta}(b) db + C, \quad (\text{C.23})$$

$$= - \int_{b \in \mathcal{B}} \int_{a \in \mathcal{A}} \int_{s \in \mathcal{S}} \log \pi_\psi(a|b) \pi_\theta(a|s) d^{\hat{\pi}_\theta}(s,b) ds da db + C, \quad (\text{C.24})$$

$$= -\mathbb{E}_{d^{\hat{\pi}_\theta}(s,b)} \left[ \int_{a \in \mathcal{A}} \log \pi_\psi(a|b) \pi_\theta(a|s) da \right] + C, \quad (\text{C.25})$$

$$= -\mathbb{E}_{d^{\hat{\pi}_\theta}(s,b)} [\mathbb{E}_{\pi_\theta(a|s)} [\log \pi_\psi(a|b)]] + C. \quad (\text{C.26})$$

As neither distribution in the expectation is a function of  $\psi$ , we can pass the derivative with respect to  $\psi$  through this objective to obtain the gradient:

$$\nabla_\psi F(\psi) = -\mathbb{E}_{d^{\hat{\pi}_\theta}(s,b)} [\mathbb{E}_{\pi_\theta(a|s)} [\nabla_\psi \log \pi_\psi(a|b)]] . \quad (\text{C.27})$$

□

Note here that in AIL  $\theta$  is held constant. In A2D we extend this by also updating the  $\theta$ , discussed later. Importantly, the gradient estimator in Equation (C.27) circumvents a critical issue. We are unable to sample from the conditional occupancy,  $d^{\hat{\pi}_\theta}(s|b)$ . However, as is common in variational methods, we instead only require samples from the joint occupancy,  $d^{\hat{\pi}_\theta}(s,b)$ . We can therefore train an approximator directly targeting the result of an intractable inference under the conditional density. Moreover, we are generally unable to sample directly from the implicit policy, and hence the variational policy provides us with a convenient method of drawing (approximate) samples from the implicit policy. Under the relatively weak assumption that the variational family is sufficiently expressive, this  $\mathbb{KL}$  divergence can be exactly minimized, and exact samples from the implicit policy are recovered. However, this does not guarantee that the implicit policy (and hence the variational policy) is optimal under the partial information. We therefore first build intermediate results by considering an identifiable process pair, where we show that we recover a sequence of updates which converges to the optimal partially observing policy,  $\hat{\pi}_{\theta^*}(a|b)$ , or its variational equivalent,  $\pi_{\psi^*}(a|b)$ . In Section C.3 we then relax the identifiability requirement, and leverage these intermediate results to derive the A2D update in Theorem 3.

## C.2.3. CONVERGENCE OF ITERATIVE AIL

We first verify the convergence of AIL for identifiable processes. We first introduce an assumption and two lemmas which provide important intermediate results and intuition, and will make the subsequent presentation of both Theorem 2 and Theorem 3 more compact. The assumption simply states that the variational family is sufficiently expressive such that the implicit policy can be replicated, and that the implicit policy is sufficiently expressive such that the optimal partially observing policy,  $\pi_{\phi^*} \in \Pi_{\Phi^*} \subseteq \Pi_{\Phi}$ , can be replicated.

The first lemma shows that the solution to an iterative procedure, optimizing the trainee under the occupancy from the trainee policy at the previous iteration, actually converges to the solution of a single equivalent “static” optimization problem, directly optimizing over the trainee policy and the corresponding occupancy. This will allow us to solve the challenging optimization over the trainee policy using a simple iterative procedure. The second lemma shows that solving this static optimization is equivalent to an optimization under the occupancy induced by the implicit policy. This will allow us to substitute the distribution under which we take expectations and will allow us to prove more complex relationships. The assumption and both lemmas are then used in Theorem 2 to show that iterative AIL will converge as required.

**Assumption 1** (Sufficiency of Policy Representations). *We assume that for any behavioral policy,  $\pi_{\eta} \in \Pi_{\Psi}$ , the variational family is sufficiently expressive such that any implicit policy,  $\hat{\pi}_{\theta} \in \hat{\Pi}_{\Theta}$ , is exactly recovered in the regions of space where the occupancy under the occupancy under the behavioral policy places mass:*

$$\min_{\psi \in \Psi} \mathbb{E}_{d^{\pi_{\eta}}(b)} [\mathbb{KL} [\hat{\pi}_{\theta}(a|b) \parallel \pi_{\psi}(a|b)]] = 0. \quad (\text{C.28})$$

We also assume that there exists an implicit policy,  $\hat{\pi}_{\theta}$ , such that an optimal POMDP policy,  $\pi_{\phi^*} \in \Pi_{\Phi^*} \subseteq \Pi_{\Phi}$  can be represented:

$$\min_{\theta \in \Theta} \mathbb{E}_{d^{\pi_{\eta}}(b)} [\mathbb{KL} [\pi_{\phi^*}(a|b) \parallel \hat{\pi}_{\theta}(a|b)]] = 0, \quad (\text{C.29})$$

and hence there is a variational policy that can represent the optimal POMDP policy in states visited under  $\pi_{\eta}$ .

The condition in Equation (C.28) (and similarly the condition in Equation (C.29)) can also be written as:

$$\exists \psi \in \Psi \quad \text{such that} \quad \hat{\pi}_{\theta}(a|b) = \pi_{\psi}(a|b), \quad \forall a \in \mathcal{A}, b \in \{b' \in \mathcal{B} \mid d^{\pi_{\eta}}(b') > 0\}. \quad (\text{C.30})$$

This condition is weaker than requiring  $\hat{\pi}_{\theta} \in \hat{\Pi}_{\Theta} \subseteq \Pi_{\Psi}$ , as this only requires that the policies are equal where the occupancy places mass. These assumptions are often made implicitly by AIL methods. We will use this assumption throughout. Note that if the condition in Equation (C.29) holds for  $\hat{\pi}_{\theta^*}$ , then the processes are identifiable.

**Lemma 2** (Convergence of Iterative Procedure). *For an MDP  $\mathcal{M}_{\Theta}$  and POMDP  $\mathcal{M}_{\Phi}$ , and implicit policy  $\pi_{\theta}$  (Definition 1), if we define a variational approximation to  $\hat{\pi}_{\theta}$ , parameterized by  $\psi$ , denoted  $\pi_{\psi} \in \hat{\Pi}_{\Psi}$ , and define:*

$$\psi_{\infty} = \lim_{k \rightarrow \infty} \arg \min_{\psi \in \Psi} \mathbb{E}_{d^{\pi_{\psi_k}}(b)} [\mathbb{KL} [\hat{\pi}_{\theta}(a|b) \parallel \pi_{\psi}(a|b)]], \quad (\text{C.31})$$

$$\psi^* = \arg \min_{\psi \in \Psi} \mathbb{E}_{d^{\pi_{\psi}}(b)} [\mathbb{KL} [\hat{\pi}_{\theta}(a|b) \parallel \pi_{\psi}(a|b)]], \quad (\text{C.32})$$

then under Assumption 1, the iterative scheme defined by Equation (C.31) converges to the solution to the optimization problem in Equation (C.32) such that:

$$\mathbb{E}_{d^{\pi_{\psi^*}}(b)} [\mathbb{KL} [\pi_{\psi^*}(a|b) \parallel \pi_{\psi_{\infty}}(a|b)]] = 0 \quad (\text{C.33})$$

*Proof.* We show this convergence by show that the total variation between  $d^{\psi^*}(b)$  and  $d^{\psi_k}(b)$ , over the set of belief states visited in Equation (C.33), denoted  $b \in \hat{\mathcal{B}} = \{b' \in \mathcal{B} \mid d^{\pi_{\psi^*}}(b') > 0\}$ , converges to zero as  $k \rightarrow \infty$ . We begin by expressing the total variation at the  $k^{\text{th}}$  iteration:

$$\sup_{b \in \hat{\mathcal{B}}} |d^{\pi_{\psi_k}}(b) - d^{\pi_{\psi^*}}(b)| = \sup_{b \in \hat{\mathcal{B}}} \left| (1 - \gamma) \sum_{t=0}^{\infty} \gamma^t q_{\pi_{\psi_k}}(b_t) - (1 - \gamma) \sum_{t=0}^{\infty} \gamma^t q_{\pi_{\psi^*}}(b_t) \right|, \quad (\text{C.34})$$

$$= (1 - \gamma) \sup_{b \in \hat{\mathcal{B}}} \left| \sum_{t=0}^{\infty} \gamma^t q_{\pi_{\psi_k}}(b_t) - \sum_{t=0}^{\infty} \gamma^t q_{\pi_{\psi^*}}(b_t) \right|, \quad (\text{C.35})$$

$$= (1 - \gamma) \sup_{b \in \mathcal{B}} \left| \sum_{t=0}^k \gamma^t q_{\pi_{\psi_k}}(b_t) + \sum_{t=k+1}^{\infty} \gamma^t q_{\pi_{\psi_k}}(b_t) - \sum_{t=0}^{\infty} \gamma^t q_{\pi_{\psi^*}}(b_t) \right|. \quad (\text{C.36})$$

where  $\gamma \in [0, 1)$ . We can then note that at the  $k^{\text{th}}$  iteration, the distribution over the first  $k$  state-belief state pairs must be identical:  $q_{\pi_{\psi_k}}(\tau_{0:k-1}) = q_{\pi_{\psi^*}}(\tau_{0:k-1})$  (recalling that  $\tau$  contains both belief state and actions).

To verify this equality consider the following inductive argument: If after a single iteration ( $k = 1$ ) we have exactly minimized the  $\mathbb{KL}$  divergence between  $\hat{\pi}_\theta$  and  $\pi_{\psi_1}$  (and hence the divergence between  $\pi_{\psi_1}$  and  $\pi_{\psi^*}$ ) for all  $b_0 \in \{b_0 \in \mathcal{B} \mid q_{\pi_{\psi_k}}(b_0) > 0\}$ . We then note that at time step zero the following equality must hold  $q_{\pi_{\psi_1}}(\tau_0) = q_{\pi_{\psi^*}}(\tau_0)$ , because the distribution over actions and the underlying dynamics are the same at the initial state and belief state. Therefore, because both the distribution over the initial state and belief state, as well as the action distributions must also be the same for  $q_{\pi_{\psi^*}}$  and  $q_{\pi_{\psi_1}}$  (i.e.  $q_{\pi_{\psi_1}}(a_0, b_0) = q_{\pi_{\psi^*}}(a_0, b_0)$ ) then necessarily we have that  $q_{\pi_{\psi_1}}(b_1) = q_{\pi_{\psi^*}}(b_1)$ .

Next, using the inductive hypothesis  $q_{\pi_{\psi_1}}(b_{k-1}) = q_{\pi_{\psi^*}}(b_{k-1})$ , we can see that provided Equation (C.28) is minimized,  $\pi_{\psi_{k-1}}(a_{k-1} | b_{k-1}) = \pi_{\psi^*}(a_{k-1} | b_{k-1})$ . This then means that again we have  $q_{\pi_{\psi_k}}(a_{k-1}, b_{k-1}) = q_{\pi_{\psi^*}}(a_{k-1}, b_{k-1})$ , which by definition gives  $q_{\pi_{\psi_k}}(b_k) = q_{\pi_{\psi^*}}(b_k)$ , which concludes our inductive proof. This allows us to make the following substitution and simplification:

$$\sup_{b \in \mathcal{B}} |d^{\pi_{\psi_k}}(b) - d^{\pi_{\psi^*}}(b)| = (1 - \gamma) \sup_{b \in \mathcal{B}} \left| \sum_{t=0}^k \gamma^t q_{\pi_{\psi^*}}(b_t) + \sum_{t=k+1}^{\infty} \gamma^t q_{\pi_{\psi_k}}(b_t) - \sum_{t=0}^{\infty} \gamma^t q_{\pi_{\psi^*}}(b_t) \right|, \quad (\text{C.37})$$

$$= (1 - \gamma) \sup_{b \in \mathcal{B}} \left| \sum_{t=k+1}^{\infty} \gamma^t q_{\pi_{\psi_k}}(b_t) - \sum_{t=k+1}^{\infty} \gamma^t q_{\pi_{\psi^*}}(b_t) \right|, \quad (\text{C.38})$$

$$= (1 - \gamma) \sup_{b \in \mathcal{B}} \left| \sum_{t=k+1}^{\infty} \gamma^t (q_{\pi_{\psi_k}}(b_t) - q_{\pi_{\psi^*}}(b_t)) \right|, \quad (\text{C.39})$$

$$\leq (1 - \gamma) \sup_{b \in \mathcal{B}} \left| \sum_{t=k+1}^{\infty} \gamma^t C \right| = C(1 - \gamma) \sum_{t=k+1}^{\infty} \gamma^t = C(1 - \gamma) \left( \frac{1}{1 - \gamma} - \frac{1 - \gamma^{k+1}}{1 - \gamma} \right) \quad (\text{C.40})$$

$$= C(1 - 1 + \gamma^{k+1}) = C\gamma^{k+1} = O(\gamma^k), \quad (\text{C.41})$$

where we assume that the maximum variation between the densities is bounded by  $C \in \mathbb{R}_+$ . Hence, as  $\gamma \in [0, 1)$ , as  $k \rightarrow \infty$  the occupancy induced by the trainee learned through the iterative procedure,  $d^{\pi_{\psi_\infty}}$ , converges to the occupancy induced by the optimal policy recovered through direct, static optimization,  $d^{\pi_{\psi^*}}$ . As a result of this, and the expressivity assumption in Equation (C.28), we can state that the iterative procedure must recover a perfect variational approximation to the implicit policy  $\hat{\pi}_\theta$ , in belief states with finite mass under  $d^{\hat{\pi}_\theta}$ .  $\square$

This lemma verifies that we can solve for a variational approximation to a particular implicit policy, defined by the static-but-difficult optimization defined in Equation (C.32), by using the tractable iterative procedure defined in Equation (C.31). However, the distribution under which we take the expectation is the trainee policy. We therefore show now that this can be replaced with the occupancy under the implicit policy, which will allow us to utilize the identifiability condition defined in the main text.

**Lemma 3** (Equivalence of Objectives). *For an MDP  $\mathcal{M}_\Theta$ , POMDP  $\mathcal{M}_\Phi$ , and implicit policy  $\hat{\pi}_\theta$  (Definition 1), if we define a variational approximation to  $\hat{\pi}_\theta$ , parameterized by  $\psi$ , denoted  $\pi_\psi \in \tilde{\Pi}_\Psi$ , and define:*

$$\psi_1^* = \arg \min_{\psi \in \Psi} \mathbb{E}_{d^{\pi_\psi}(b)} [\mathbb{KL}[\hat{\pi}_\theta(a|b) \parallel \pi_\psi(a|b)]], \quad (\text{C.42})$$

$$\psi_2^* = \arg \min_{\psi \in \Psi} \mathbb{E}_{d^{\hat{\pi}_\theta}(b)} [\mathbb{KL}[\hat{\pi}_\theta(a|b) \parallel \pi_\psi(a|b)]], \quad (\text{C.43})$$

then, under Assumption 1, we are able to show that:

$$\mathbb{E}_{d^{\pi_{\psi_2^*}}(b)} [\mathbb{KL}[\psi_2^*(a|b) \parallel \psi_1^*(a|b)]] = 0 \quad (\text{C.44})$$

*Proof.* We show this result by way of contradiction. First assume that there exists some  $t \in \mathbb{N}$  such that  $q_{\hat{\pi}_\theta}(b_t) \neq q_{\pi_{\psi_k}}(b_t)$ . As a result of Assumption 1 we know that:

$$\min_{\psi \in \Psi} \mathbb{E}_{d^{\pi_\psi}(b)} [\mathbb{KL} [\hat{\pi}_\theta(a|b) \parallel \pi_\psi(a|b)]] = 0. \quad (\text{C.45})$$

In a similar fashion to Lemma 2, we can first note that because the initial state distribution is independent of the policy,  $q_{\hat{\pi}_\theta}(b_0) = q_{\pi_\psi}(b_0)$ . Then because both Equation (C.42) and (C.43) target the same density, by Assumption 1 we have again that  $q_{\hat{\pi}_\theta}(b_0)\hat{\pi}_\theta(a_0|b_0) = q_{\pi_\psi}(b_0)\pi_\psi(a_0|b_0)$ . Because the dynamics are the same for both  $q_{\pi_\psi}$  and  $q_{\hat{\pi}_\theta}$ , this result directly implies that  $q_{\hat{\pi}_\theta}(b_1) = q_{\pi_\psi}(b_1)$ .

Inductively extending this to  $t - 1$ , we have that  $q_{\hat{\pi}_\theta}(b_{t-1}) = q_{\pi_\psi}(b_{t-1})$ , and further that our action distribution again satisfies  $\pi_{\psi_t}(a_{t-1}|b_{t-1}) = \hat{\pi}_\theta(a_{t-1}|b_{t-1})$  due to Assumption 1. Here we again have that  $\pi_{\psi_t}(a_{t-1}|b_{t-1})q_{\pi_\psi}(b_{t-1}) = \hat{\pi}_\theta(a_{t-1}|b_{t-1})q_{\hat{\pi}_\theta}(b_{t-1})$ , which directly implies that  $q_{\hat{\pi}_\theta}(b_t) = q_{\pi_\psi}(b_t)$  must also hold. However this contradicts our assumption that  $\exists t \in \mathbb{N}$  such that  $q_{\hat{\pi}_\theta}(b_t) \neq q_{\pi_{\psi_k}}(b_t)$ . Thus under the assumptions stated above,  $q_{\hat{\pi}_\theta}(b_t) = q_{\pi_\psi}(b_t)$  for all  $t$ , and by extension,  $d^{\hat{\pi}_\theta}(b) = d^{\pi_{\psi^*}}(b)$ , where  $\pi_{\psi^*}$  represents a solution to the right hand side of Equation (C.43).  $\square$

This lemma allows us to exchange the distribution under which we take expectations. We can now use Assumption 1, Lemma 2 and Lemma 3 to show that for an identifiable process pair an iterative AIL procedure converges to the correct POMDP policy as desired.

**Theorem 2** (Convergence of AIL, expanded from Section 4). *Consider an identifiable MDP-POMDP pair  $(\mathcal{M}_\Theta, \mathcal{M}_\Phi)$ , with optimal expert policy,  $\pi_{\theta^*}$ , and optimal partially observing policy  $\pi_{\phi^*} \in \Pi_{\Phi^*} \subseteq \Pi_\Phi$ . For a variational policy  $\pi_\psi \in \Pi_\Psi$ , and assuming Assumption 1 holds, the following iterative procedure:*

$$\psi_{k+1} = \arg \min_{\psi \in \Psi} \mathbb{E}_{d^{\pi_{\psi_k}}(s,b)} [\mathbb{KL} [\pi_{\theta^*}(a|s) \parallel \pi_\psi(a|b)]], \quad (\text{C.46})$$

*converges to parameters  $\psi^* = \lim_{k \rightarrow \infty} \psi_k$  that define a policy equal to an optimal partially observing policy in visited regions of state-space:*

$$\mathbb{E}_{d^{\pi_{\phi^*}}(b)} [\mathbb{KL} [\pi_{\phi^*}(a|b) \parallel \pi_{\psi^*}(a|b)]] = 0 \quad (\text{C.47})$$

*Proof.* For brevity, we present this proof for the case that there is a unique optimal parameter value,  $\psi^*$ . However, this is not a *requirement*, and can easily be relaxed to consider a set of equivalent parameters,  $\psi_{1:N}^*$ , that yield the same policy over the relevant occupancy distribution, i.e.  $\pi_{\psi_1^*}(a|b) = \dots = \pi_{\psi_N^*}(a|b) \forall b \in \hat{B}$ . In this case, we would instead require that the  $\mathbb{KL}$  divergence between the resulting policies is zero (analogous to Equation (C.47)), as opposed to requiring that the parameters recovered are *equal* to  $\psi^*$ . However, including this dramatically complicates the exposition and hence we do not include such a proof here. We begin by considering the limiting behavior of Equation (C.46) as  $k \rightarrow \infty$ :

$$\psi^* = \lim_{k \rightarrow \infty} \arg \min_{\psi \in \Psi} \mathbb{E}_{d^{\pi_{\psi_k}}(s,b)} [\mathbb{KL} [\pi_{\theta^*}(a|s) \parallel \pi_\psi(a|b)]]. \quad (\text{C.48})$$

Application of Theorem 1 to replace the expert policy with the implicit policy yields:

$$= \lim_{k \rightarrow \infty} \arg \min_{\psi \in \Psi} \mathbb{E}_{d^{\pi_{\psi_k}}(b)} [\mathbb{KL} [\hat{\pi}_{\theta^*}(a|b) \parallel \pi_\psi(a|b)]]. \quad (\text{C.49})$$

Application of Lemma 2 to Equation (C.49) then recovers the limiting behavior as  $k \rightarrow \infty$ :

$$= \arg \min_{\psi \in \Psi} \mathbb{E}_{d^{\pi_\psi}(b)} [\mathbb{KL} [\hat{\pi}_{\theta^*}(a|b) \parallel \pi_\psi(a|b)]]. \quad (\text{C.50})$$

Application of Lemma 3 to change the distribution under which the expectation is taken yields:

$$= \arg \min_{\psi \in \Psi} \mathbb{E}_{d^{\hat{\pi}_{\theta^*}}(b)} [\mathbb{KL} [\hat{\pi}_{\theta^*}(a|b) \parallel \pi_\psi(a|b)]], \quad (\text{C.51})$$

Identifiability then directly implies that the implicit policy defined by the optimal expert policy *is* an optimal partially observing policy:

$$\mathbb{E}_{d^{\pi_{\phi^*}}(b)} [\mathbb{KL} [\pi_{\phi^*}(a|b) \parallel \hat{\pi}_{\theta^*}(a|b)]] = 0, \quad (\text{C.52})$$



and therefore we can replace  $\hat{\pi}_{\theta^*}$  with  $\pi_{\phi^*}$  in Equation (C.51) to yield:

$$\psi^* = \arg \min_{\psi \in \Psi} \mathbb{E}_{d^{\pi_{\phi^*}}(b)} [\mathbb{KL} [\pi_{\phi^*}(a|b) \parallel \pi_{\psi}(a|b)]], \quad (\text{C.53})$$

Finally, under Assumption 1, the expected  $\mathbb{KL}$  divergence in Equation (C.51) can be exactly minimized, such that:

$$\mathbb{E}_{d^{\pi_{\phi^*}}(b)} [\mathbb{KL} [\pi_{\phi^*}(a|b) \parallel \pi_{\psi^*}(a|b)]] = 0 \quad (\text{C.54})$$

□

This proof shows that, if Assumption 1 holds and for an identifiable MDP-POMDP pair, we can use a convenient iterative scheme defined in Equation (C.46) to recover an optimal trainee policy that is equivalent to an optimal partially observing policy. This iterative process is more tractable than the directly solving the equivalent static optimization; instead gathering trajectories under the current trainee policy, regressing the trainee onto the expert policy at each state, and then rolling out under the new trainee policy until convergence. However, assuming that processes are identifiable is a *very* restrictive assumption. This fact motivates our A2D algorithm, which exploits AIL to recover an optimal partially observing policy for any process pair by adaptively modifying the expert that is imitated by the trainee.

### C.3. A2D Proofs

In this section we provide the proofs, building on the results given above, that underpin our A2D method and facilitate robust exploitation of AIL in non-identifiable process pairs. We begin this section by giving a proof of the bound described in Equations (21)-(22). We then give proofs of the A2D gradient estimators given in Equations (24) and (25). We then conclude with a proof of Theorem 3, which closely follows the proof for Theorem 2, and provides the theoretical underpinning of the A2D algorithm. We conclude by discussing briefly the practical repercussions of this result, as well as some additional assumptions that can be made to simplify the analysis.

#### C.3.1. OBJECTIVES AND GRADIENTS ESTIMATORS

We begin by expanding on the policy gradient bound given in Equations (21)-(22).

**Lemma 4** (Policy gradients bound, c.f. Section 5, Equations (21)-(22)). *Consider an expert policy,  $\pi_{\theta}$ , and a trainee policy learned through  $\mathbb{KL}$ -minimization,  $\pi_{\psi}$ , targeting the implicit policy,  $\hat{\pi}_{\theta}$ . If Equation (C.29) in Assumption 1 holds, the following bound holds:*

$$\max_{\theta \in \Theta} J_{\psi}(\theta) = \max_{\theta \in \Theta} \mathbb{E}_{\hat{\pi}_{\theta}(a|b)d^{\pi_{\psi}}(b)} [Q^{\pi_{\psi}}(a, b)] \leq \max_{\theta \in \Theta} \mathbb{E}_{\hat{\pi}_{\theta}(a|b)d^{\pi_{\psi}}(b)} [Q^{\hat{\pi}_{\theta}}(a, b)] = \max_{\theta \in \Theta} J(\theta). \quad (\text{C.55})$$

*Proof.* For a more extensive discussion on this form of policy improvement we refer the reader to [Agarwal et al. \(2020\)](#); [Bertsekas & Tsitsiklis \(1991\)](#); [Bertsekas \(2011\)](#). Assumption 1 states that the optimal partially observing policy (or policies) is representable by an implicit policy for any occupancy distribution. We denote the optimal value function as  $V^*(b)$ , where this value function is realizable by the implicit policy. Considering the right hand side of Equation (C.55), we can write, by definition, the following equality:

$$\max_{\theta \in \Theta} \mathbb{E}_{\hat{\pi}_{\theta}(a|b)d^{\pi_{\psi}}(b)} [Q^{\hat{\pi}_{\theta}}(a, b)] = \max_{\theta \in \Theta} \mathbb{E}_{d^{\pi_{\psi}}(b)} \left[ \mathbb{E}_{\hat{\pi}_{\theta}(a|b)} \left[ \mathbb{E}_{p(b'|a,b)} [r(b, a, b')] + \gamma \mathbb{E}_{p(b'|a,b)} [V^{\hat{\pi}_{\theta}}(b')] \right] \right] \quad (\text{C.56})$$

$$= \max_{\theta \in \Theta} \mathbb{E}_{d^{\pi_{\psi}}(b)} \left[ \mathbb{E}_{\hat{\pi}_{\theta}(a|b)} \left[ \mathbb{E}_{p(b'|a,b)} [r(b, a, b')] + \gamma \mathbb{E}_{p(b'|a,b)} [V^*(b')] \right] \right] \quad (\text{C.57})$$

We then repeat this for the expression on the left side of Equation (C.55), noting that instead of equality there is an inequality, as by definition the value function induced by  $\pi_{\psi}(a|b)$ , denoted  $V^{\pi_{\psi}}(b)$  cannot be *better* than  $V^*(b)$ :

$$V^{\pi_{\psi}}(b) \leq V^*(b) \quad \forall b \in \left\{ \tilde{b} \in \mathcal{B} \mid d^{\pi_{\psi}}(\tilde{b}) > 0 \right\}, \quad (\text{C.58})$$

$$\max_{\theta \in \Theta} \mathbb{E}_{\hat{\pi}_{\theta}(a|b)d^{\pi_{\psi}}(b)} [Q^{\pi_{\psi}}(a, b)] = \max_{\theta \in \Theta} \mathbb{E}_{d^{\pi_{\psi}}(b)} \left[ \mathbb{E}_{\hat{\pi}_{\theta}(a|b)} \left[ \mathbb{E}_{p(b'|a,b)} [r(b, a, b')] + \gamma \mathbb{E}_{p(b'|a,b)} [V^{\pi_{\psi}}(b')] \right] \right] \quad (\text{C.59})$$

$$\leq \max_{\theta \in \Theta} \mathbb{E}_{d^{\pi_\psi}(b)} \left[ \mathbb{E}_{\hat{\pi}_\theta(a|b)} \left[ \mathbb{E}_{p(b'|a,b)} [r(b, a, b')] + \gamma \mathbb{E}_{p(b'|a,b)} [V^*(b')] \right] \right], \quad (\text{C.60})$$

and hence the inequality originally stated in Equation (C.55) must hold.  $\square$

This form of improvement over a behavioral policy is well studied in the approximate dynamic programming literature (Bertsekas, 2019), and is a useful tool in analyzing classical methods such as approximate policy iteration. As was discussed in Section 5, it is also implicitly used in many policy gradient algorithms to avoid differentiating through the Q function, especially when a differentiable Q function is not available. In these cases (i.e. Schulman et al. (2017; 2015a;b); Williams (1992)) the behavioral policy is defined as the policy under which samples are gathered for Q function estimation. Then, as in the classical policy gradient theorem (Bertsekas, 2019; Sutton, 1992; Williams, 1992), the discounted sum of rewards ahead does not need to be differentiated through. We can then exploit this lower bound to construct an estimator of the gradient of the expert parameters with respect to the reward garnered by the implicit policy.

**Lemma 5** (A2D Q-based gradient estimator, c.f. Section 5, Equation (24)). *For an expert policy,  $\pi_\theta$ , and a trainee policy learned through  $\mathbb{KL}$ -minimization,  $\pi_\psi$ , targeting the implicit policy,  $\hat{\pi}_\theta$ , we can transform the following policy gradient update applied directly the lower trainee policy bound in Equation (C.55):*

$$\nabla_\theta J_\psi(\theta) = \nabla_\theta \mathbb{E}_{\hat{\pi}_\theta(a|b)d^{\pi_\psi}(b)} [Q^{\pi_\psi}(a, b)], \quad (\text{C.61})$$

into a policy gradient update applied to the expert:

$$\nabla_\theta J_\psi(\theta) = \mathbb{E}_{d^{\pi_\psi}(s,b)} \left[ \mathbb{E}_{\pi_\theta(a|s)} [Q^{\pi_\psi}(a, b) \nabla_\theta \log \pi_\theta(a|s)] \right], \quad (\text{C.62})$$

*Proof.* To prove this we simply expand and rearrange Equation (C.61):

$$\nabla_\theta J_\psi(\theta) = \nabla_\theta \mathbb{E}_{\hat{\pi}_\theta(a|b)d^{\pi_\psi}(b)} [Q^{\pi_\psi}(a, b)], \quad (\text{C.63})$$

$$= \nabla_\theta \int_{b \in \mathcal{B}} \int_{a \in \mathcal{A}} Q^{\pi_\psi}(a, b) \hat{\pi}_\theta(a|b) da d^{\pi_\psi}(b) db, \quad (\text{C.64})$$

$$= \nabla_\theta \int_{b \in \mathcal{B}} \int_{a \in \mathcal{A}} Q^{\pi_\psi}(a, b) \int_{s \in \mathcal{S}} \pi_\theta(a|s) d^{\pi_\psi}(s|b) ds da d^{\pi_\psi}(b) db, \quad (\text{C.65})$$

$$= \nabla_\theta \int_{s \in \mathcal{S}} \int_{b \in \mathcal{B}} \int_{a \in \mathcal{A}} Q^{\pi_\psi}(a, b) \pi_\theta(a|s) d^{\pi_\psi}(s, b) da ds db, \quad (\text{C.66})$$

$$= \mathbb{E}_{d^{\pi_\psi}(s,b)} \left[ \nabla_\theta \int_{a \in \mathcal{A}} Q^{\pi_\psi}(a, b) \pi_\theta(a|s) da \right], \quad (\text{C.67})$$

$$= \mathbb{E}_{d^{\pi_\psi}(s,b)} \left[ \nabla_\theta \mathbb{E}_{\pi_\theta(a|s)} [Q^{\pi_\psi}(a, b)] \right], \quad (\text{C.68})$$

$$= \mathbb{E}_{d^{\pi_\psi}(s,b)} \left[ \mathbb{E}_{\pi_\theta(a|s)} [Q^{\pi_\psi}(a, b) \nabla_\theta \log \pi_\theta(a|s)] \right], \quad (\text{C.69})$$

$\square$

The implementation of A2D given in Equation (24), when not directly learning the Q function, then extends this by using an importance weighted version of the inner expectation. This allows us to instead weight actions sampled under the current trainee policy,  $\pi_\psi$ , without biasing the gradient estimator. The standard A2D implementation in Equation (25) is then in terms of advantage, which is the Q function with the value function subtracted as a baseline.

**Lemma 6** (A2D Advantage-based gradient estimator, c.f. Section 5, Equation (25)). *We can construct a gradient estimator from Equation (C.69) that uses the advantage by subtracting the value function as a baseline (Sutton, 1992; Williams, 1992; Bertsekas, 2019):*

$$\nabla_\theta J_\psi(\theta) = \mathbb{E}_{d^{\pi_\psi}(s,b)} \left[ \mathbb{E}_{\pi_\theta(a|s)} [Q^{\pi_\psi}(a, b) \nabla_\theta \log \pi_\theta(a|s)] \right], \quad (\text{C.70})$$

$$= \mathbb{E}_{d^{\pi_\psi}(s,b)} \left[ \mathbb{E}_{\pi_\theta(a|s)} [(Q^{\pi_\psi}(a, b) - V^{\pi_\psi}(b)) \nabla_\theta \log \pi_\theta(a|s)] \right]. \quad (\text{C.71})$$

*Proof.* It is sufficient to show that:

$$\mathbb{E}_{d^{\pi_{\psi}}(s,b)} \left[ \mathbb{E}_{\pi_{\theta}(a|s)} \left[ V^{\hat{\pi}_{\theta}}(b) \nabla_{\theta} \log \pi_{\theta}(a|s) \right] \right] = 0, \quad (\text{C.72})$$

which can be shown easily as:

$$\mathbb{E}_{d^{\pi_{\psi}}(s,b)} \left[ \mathbb{E}_{\pi_{\theta}(a|s)} \left[ V^{\hat{\pi}_{\theta}}(b) \nabla_{\theta} \log \pi_{\theta}(a|s) \right] \right] = \mathbb{E}_{d^{\pi_{\psi}}(s,b)} \left[ V^{\hat{\pi}_{\theta}}(b) \mathbb{E}_{\pi_{\theta}(a|s)} \left[ \nabla_{\theta} \log \pi_{\theta}(a|s) \right] \right] \quad (\text{C.73})$$

$$= \mathbb{E}_{d^{\pi_{\psi}}(s,b)} \left[ V^{\hat{\pi}_{\theta}}(b) \int_{a \in \mathcal{A}} \nabla_{\theta} \pi_{\theta}(a|s) da \right], \quad (\text{C.74})$$

$$= \mathbb{E}_{d^{\pi_{\psi}}(s,b)} \left[ V^{\hat{\pi}_{\theta}}(b) \nabla_{\theta} \int_{a \in \mathcal{A}} \pi_{\theta}(a|s) da \right], \quad (\text{C.75})$$

$$= \mathbb{E}_{d^{\pi_{\psi}}(s,b)} \left[ V^{\hat{\pi}_{\theta}}(b) \nabla_{\theta} 1 \right] = 0, \quad (\text{C.76})$$

Noting that this is an example of the *baseline* trick used throughout RL (Sutton, 1992; Williams, 1992; Bertsekas, 2019).  $\square$

This allows us to construct a gradient estimator using the advantage, which in conventional RL, is observed to reduce the variance of the gradient estimator compared to directly using the Q values.

We are now able to prove an exact form of the A2D update. This proof is similar to Theorem 2, however, no longer assumes identifiability of the POMDP-MDP process pair by instead updating the expert at each iteration.

### C.3.2. THEOREM 3

**Theorem 3** (Convergence of Exact A2D, reproduced from Section 5). *Under exact intermediate updates to the expert policy (see Equation (C.78)), and Assumption 1, the following iteration converges to an optimal partially observed policy  $\pi_{\psi^*}(a|b) \in \Pi_{\phi}$ :*

$$\psi_{k+1} = \arg \min_{\psi \in \Psi} \mathbb{E}_{d^{\pi_{\psi_k}}(s,b)} \left[ \mathbb{KL} \left[ \pi_{\hat{\theta}_k^*}(a|s) \parallel \pi_{\psi}(a|b) \right] \right], \quad (\text{C.77})$$

$$\text{where } \hat{\theta}_k^* = \arg \max_{\theta \in \Theta} \mathbb{E}_{d^{\pi_{\psi_k}}(b) \hat{\pi}_{\theta}(a|b)} \left[ Q^{\hat{\pi}_{\theta}}(a, b) \right]. \quad (\text{C.78})$$

*Proof.* We will again, for ease of exposition assume that a unique optimal policy exists, as in Theorem 2. We again reinforce that this is not a *requirement*. Extending this proof to include multiple optimal partially observable policies only requires that we reason about the  $\mathbb{KL}$  divergence between  $\pi_{\psi_k}$  and  $\pi_{\psi^*}$  at each step in the proof, instead of showing that the optimal parameters are equal. This alteration is technically simple, but is algebraically and notationally onerous. Similar to Theorem 2, we begin by examining the limiting behavior of Equation (C.77) as  $k \rightarrow \infty$ , and apply Theorem 1 to replace the expert policy with the implicit policy:

$$\psi^* = \lim_{k \rightarrow \infty} \arg \min_{\psi \in \Psi} \mathbb{E}_{d^{\pi_{\psi_k}}(s,b)} \left[ \mathbb{KL} \left[ \pi_{\hat{\theta}_k^*}(a|s) \parallel \pi_{\psi}(a|b) \right] \right], \quad (\text{C.79})$$

$$= \lim_{k \rightarrow \infty} \arg \min_{\psi \in \Psi} \mathbb{E}_{d^{\pi_{\psi_k}}(b)} \left[ \mathbb{KL} \left[ \hat{\pi}_{\hat{\theta}_k^*}(a|b) \parallel \pi_{\psi}(a|b) \right] \right] \quad (\text{C.80})$$

We can then apply a direct extension of Lemma 2, where the parameters of the expert policy are also updated in each iteration of the  $\mathbb{KL}$  minimization, now denoted  $\hat{\theta}^*(\psi)$ . The induction in Lemma 2 then proceeds as before. Application of this extended Lemma 2 yields:

$$\psi^* = \lim_{k \rightarrow \infty} \arg \min_{\psi \in \Psi} \mathbb{E}_{d^{\pi_{\psi_k}}(b)} \left[ \mathbb{KL} \left[ \hat{\pi}_{\hat{\theta}_k^*}(a|b) \parallel \pi_{\psi}(a|b) \right] \right], \quad (\text{C.81})$$

$$= \arg \min_{\psi \in \Psi} \mathbb{E}_{d^{\pi_{\psi}}(b)} \left[ \mathbb{KL} \left[ \hat{\pi}_{\hat{\theta}^*(\psi)}(a|b) \parallel \pi_{\psi}(a|b) \right] \right], \quad \text{where } \hat{\theta}^*(\psi) = \arg \max_{\theta \in \Theta} \mathbb{E}_{d^{\pi_{\psi}}(b) \hat{\pi}_{\theta}(a|b)} \left[ Q^{\hat{\pi}_{\theta}}(a, b) \right] \quad (\text{C.82})$$

We can then apply a similarly extended a version of Lemma 3, by using the same logic to allow the parameters of the expert policy to be updated as a function of  $\psi$  in the  $\mathbb{KL}$  minimization. Now  $\hat{\theta}^*(\psi)$  is defined as the expectation under the optimal

POMDP policy. To clarify, this is, of course, intractable; however, here we are deriving what the tractable iterative scheme outlined in Equation (C.77) converges to, and hence we never actually need to evaluate  $\hat{\theta}^*(\psi)$  as it is defined in Equation (C.82). Application of this extended lemma yields:

$$\psi^* = \arg \min_{\psi \in \Psi} \mathbb{E}_{d^{\pi_{\psi}}(b)} \left[ \mathbb{KL} \left[ \hat{\pi}_{\hat{\theta}^*(\psi)}(a|b) \parallel \pi_{\psi}(a|b) \right] \right], \quad (\text{C.83})$$

$$= \arg \min_{\psi \in \Psi} \mathbb{E}_{d^{\pi_{\phi^*}}(b)} \left[ \mathbb{KL} \left[ \hat{\pi}_{\hat{\theta}^*(\psi)}(a|b) \parallel \pi_{\psi}(a|b) \right] \right], \quad \text{where } \hat{\theta}^*(\psi) = \arg \max_{\theta \in \Theta} \mathbb{E}_{d^{\pi_{\phi^*}}(b) \hat{\pi}_{\theta}(a|b)} \left[ Q^{\hat{\pi}_{\theta}}(a, b) \right] \quad (\text{C.84})$$

Lastly, Assumption 1 states that  $\pi_{\phi^*} \in \hat{\Pi}_{\hat{\theta}^*}$ , and so we can replace  $\hat{\pi}_{\hat{\theta}^*}$  with the optimal partially observing policy  $\pi_{\phi^*}$ . As a result, we have shown that we are implicitly solving a symmetric imitation learning problem, imitating the optimal partially observing policy:

$$\psi^* = \arg \min_{\psi \in \Psi} \mathbb{E}_{d^{\pi_{\phi^*}}(b)} \left[ \mathbb{KL} \left[ \hat{\pi}_{\hat{\theta}^*(\psi)}(a|b) \parallel \pi_{\psi}(a|b) \right] \right], \quad (\text{C.85})$$

$$= \arg \min_{\psi \in \Psi} \mathbb{E}_{d^{\pi_{\phi^*}}(b)} \left[ \mathbb{KL} \left[ \pi_{\phi^*}(a|b) \parallel \pi_{\psi}(a|b) \right] \right], \quad (\text{C.86})$$

where this optima can be achieved by our variational policy, yielding the initially states result:

$$\psi^* = \lim_{k \rightarrow \infty} \arg \min_{\psi \in \Psi} \mathbb{E}_{d^{\pi_{\psi_k}}(s, b)} \left[ \mathbb{KL} \left[ \pi_{\hat{\theta}_k^*}(a|s) \parallel \pi_{\psi}(a|b) \right] \right] = \arg \min_{\psi \in \Psi} \mathbb{E}_{d^{\pi_{\phi^*}}(b)} \left[ \mathbb{KL} \left[ \pi_{\phi^*}(a|b) \parallel \pi_{\psi}(a|b) \right] \right] \quad (\text{C.87})$$

Directly performing the imitation in the right hand side of Equation (C.87), although practically intractable, is guaranteed to recover a performant trainee. We have therefore shown that the iterative procedure outlined in Equations (C.77) and (C.78) recovers a trainee that is equivalent to an optimal partially observing policy as desired.  $\square$

We conclude by noting that if we assume that  $d^{\pi_{\psi}} > 0$  for all  $\pi_{\psi} \in \Pi_{\psi}$ , then each of the steps given in Theorems 2 and 3 can be shown trivially. If we assume at each iteration we successfully minimize the  $\mathbb{KL}$  divergence, we obtain a variational policy which perfectly matches the updated expert everywhere. In Theorem 2 this directly implies the result, and by definition the algorithm must have converged after just a single iteration. In Theorem 3, we need only note that the arg max that produces the updated expert policy parameters must itself by definition match the optimal partially observed policy everywhere, and thus Theorem 3 collapses to the same logic from Theorem 2.

### C.3.3. DISCUSSION

In this section we presented a derivation of exact A2D, where the expert is defined through the exact internal maximization step defined in Equation (C.78). We include these derivations to show the fundamental limitations of imitation learning and thus A2D under ideal settings. Exactly performing this maximization is difficult unto itself, and therefore the A2D algorithm presented in Algorithm 1 simply assumes that this maximization is performed sufficiently accurately to produce meaningful progress in policy space. Although we note that empirically A2D is robust to inexact updates, we defer the challenging task of formally and precisely quantifying the convergence properties of A2D under inexact internal updates to future work.

## D. Experimental Configurations

### D.1. Gridworld

We implemented both gridworld environments by adapting the *MiniGrid* environment provided by [Chevalier-Boisvert et al. \(2018\)](#). For both gridworld experiments, the image is rendered as a  $42 \times 42$  RGB image. The agent has four actions available, moving in each of the compass directions. Each movement incurs a reward of  $-2$ , hitting the weak patch of ice or tiger incurs a reward of  $-50$ , and reaching the goal incurs a reward of  $20$ . Pushing the button in Tiger Door is free, but effectively costs  $4$  due to its position, or  $2$  in the Q-function experiments. Policy performance is evaluated every 5 steps by sampling 2000 interactions under the stochastic policy. A discount factor of  $\gamma = 0.995$  was used,  $\lambda = 0.95$  in the GAE calculation ([Schulman et al., 2015b](#)). An upper limit of  $T = 200$  is placed on the time horizon.

For the expert we use a two layer MLP, with 64 hidden units in each layer, outputting the log-probabilities of each action. Agent/trainee policies use a two layer convolutional policy, each with 32 filters, mapping to a flat hidden state with 50 hidden units, being used as input into a two layer MLP, each with 64 hidden units, outputting the log-probabilities of each action. In TRPO, the expert policy is updated using a trust region allowing a maximum KL-divergence of 0.01. The value function is a two layer MLP, each with 64 hidden units, targeting the sum of rewards ahead by minimizing the mean squared error. 32 batches are constructed from the rollout and are used to update the value function using ADAM ([Kingma & Ba, 2014](#)) with a learning rate of  $7e - 4$ , for ten whole epochs. L2 regularization is applied to all networks, with a coefficient of 0.001.

The expert policy used in AIL (asymmetric DAGger, AD) is the result of applying TRPO on the MDP using the above hyperparameters. We find that the MDP converges within approximately 80,000 environment interactions, and so we begin the AD line at this value. For both A2D and AD, a replay buffer of size 5,000 was used. The KL-divergence between the expert and trainee action distributions is minimized by performing stochastic gradient descent, using ADAM with a learning rate of  $3e - 4$ , using a batch size of 64. In AD,  $\beta$  is annealed to zero after the first time step (as recommended by [Ross et al. \(2011\)](#)). For the experiments in [Figure 4](#), an entropy regularizer is applied directly to the advantages computed, with coefficient 10. For the experiments in [Appendix Figure B.4](#) an entropy regularizer of 0.001 is applied directly to the surrogate loss. We did not find either one of these configurations to be noticeably more effective. Asymmetric reinforcement learning takes the compact and omniscient state representation ( $s_t$ ) as input. When training the encoder, we rollout under a trained MDP, collect the trajectories generated by 10,000 environment interactions. An encoder that takes the images as input and targets the true state is learned by regressing the predictions on to the true state. We also start this curve at the 80,000 interactions required to train the expert from which the encoder is learned. We confirm for both pretrained encoders and AD that the policy and encoder class can represent the required policies and transforms when conditioned on fully observed image-based input.

For investigating the use of Q function approximators, we use a  $\lambda$  value of zero to enforce reliance on the function approximators ([Schulman et al., 2015b](#)). Q functions are learned using the same method as value functions, except targeting the expected sum of rewards ahead conditioned on both state and action, with a learning rate  $3e - 4$ . We also use TRPO with a trust region KL-divergence of 0.001. In the PPO experiments in [Figure B.1](#) we use a batch size of 32 and a learning rate of  $7e - 4$  when updating the policy. We also decay  $\beta$  as a faster rate of 0.8.

### D.2. CARLA Experiments

We implemented our autonomous vehicle experiment using CARLA ([Dosovitskiy et al., 2017](#)). This scenario roughly speaking represents a car driving forward at the speed limit, while avoiding a pedestrian which will run out from behind a vehicle 50% of the time, at a variable speed. There are a total of 10 waypoints, indicating the path the vehicle should take as produced by an external path planner. We enforce that the scenario will end prematurely if one of the following occurs: a time limit of 90 time-steps is reached, a collision with a static object, a lane invasion occurs, if a waypoint is not gathered within 35 time-steps, or, the car’s path is not within a certain distance of the nearest waypoint. We found that inclusion of these premature endings was crucial for efficient learning. The reward surface for this problem is generated using a PID controller which is computed using an example nominal trajectory. The reward at any given time-step is defined as the product of the absolute difference between the agents actions and the optimal actions by a low-level PID controller to guide the vehicle to the next waypoint, and is bounded to lie in  $[0, 1]$ .

For the expert policy used both in AIL and A2D, we use a two layer MLP with 64 hidden units and ReLU activations. The agent and trainee policies use an image encoder ([Laskin et al., 2020a;b](#); [Yarats et al., 2021](#)), followed by the same MLP architecture as the expert policy to generate actions. The RL algorithm used in both the expert and agent RL updates is

PPO Schulman et al. (2017) with generalized advantage estimation (GAE) Schulman et al. (2015b). We detach the encoder during the policy update and learn the encoder during the value function update (Laskin et al., 2020a;b; Yarats et al., 2021). In A2D we use the MLP defined above for the expert policy. The trainee policy and value functions use a common encoder, updated during the trainees value update and frozen during the policy update, and the MLP defined above as the policy head or value head network. For all algorithms we used a batch size of 64 in both the PPO policy update, value function update, and the imitation learning update. As in the previous experiments, in the imitation learning step, we iterate through all data seen and stored in the replay buffer. Unlike the previous experiments, we found that starting the  $\beta$  parameter at zero produced faster convergence.

We performed a coarse-grained hyperparameter search using the Bayesian optimization routine provided by the experimental control and logging software *Weights & Biases* (Biewald, 2020). This allows us to automate hyperparameter search and distribute experimental results for more complex experiments in a reproducible manner. Each method was provided approximately the same amount of search time, evaluating at least 60 different hyperparameter settings. The optimal settings were then improved manually over the course of approximately 5 further tests. We score each method and hyperparameter setting using a running average of the reward over the previous 25 evaluation steps, and used early stopping if a run consistently performed poorly. For a detailed list of parameters used in this experiment see the attached yaml files.

Each algorithm uses different learning rates and combinations of environment steps between updates. For example, we found that all AIL algorithms performed best when taking 10 steps between updates, RL in the expert tended to work better by taking more steps in between updates ( $\approx 400$ ) with a larger step-size  $\approx 4 \cdot 10^{-4}$ , where the agents RL updates favored fewer steps  $\approx 75$  with smaller steps  $7 \cdot 10^{-5}$ . For all algorithms 4 parallel environments were run concurrently, as this was observed to improve performance across all algorithms. This was especially the case for the RL methods, which relied on more samples to accurately compute the advantage.

We note that there is a point of diminishing returns for PPO (Schulman et al., 2017) specifically (Engstrom et al., 2020), where policy learning degrades as the number of examples per update increases. Even though the advantage becomes progressively more accurate with increasing sample size, the mini-batch gradient decent procedure in PPO eventually leads to off-policy behavior that can be detrimental to learning. We also found that pre-generating a number of trajectories and pretraining the value function tended to improve performance for both A2D, as well as the compact expert RL algorithm. For A2D specifically, this ensured that the replay buffer for imitation learning was reasonably large prior to learning in the expert. This ensures that for any given update, the agent tends to be close to the expert policy, ensuring that the "off-policy" RL update is not too severely destabilized through importance weighting. To further improve this, we also introduced delayed policy updates, which further reduced the divergence between expert and the agent in A2D. In both A2D and the RL setups, this also helped ensure that the value function is always converging faster than the policy, ensuring that the error in the resulting advantage estimates are low.

## E. Additional Related Work

We now present a comprehensive review of existing literature not already covered. Exploiting asymmetric learning to accelerate learning has been explored in numerous previous work under a number of different frameworks, application domains, and levels of theoretical analysis.

The notion of using fully observed states unavailable at deployment time is often referred to as exploiting “privileged information” (Vapnik & Vashist, 2009; Lambert et al., 2018). For clarity, we refer to the expert as having access to privileged information, and the agent as only having access to a partial observation. We note that the use of the term “expert” does not imply that this policy is necessarily optimal under the MDP. Indeed, in A2D, the expert is co-trained with the agent, such that the expert is approximately a uniform random distribution at the start of the learning procedure. The term privileged information is more general than simply providing the world state, and may include additional loss terms or non-trivial transforms of the world state that expedite learning the agent. In this work, we exclusively consider the most general scenario where the privileged information is the full world state. However, there is nothing precluding defining an extended state space to include hand-designed features extracted from the state, or, using additional, hand crafted reward shaping terms when learning (or adapting) the expert.

### E.1. Encodings

The first use-case we examine is probably the simplest, and the most widely studied. Asymmetric information is used to learn an encoding of the observation that reduces the dimensionality while retaining information. Standard reinforcement learning approaches are then employed freezing this encoding. Two slight variations on this theme exist. In the first approach, an MDP policy is learned to generate rollouts conditioned on omniscient information, and an encoder is learned on state-observation pairs visited during these rollouts (Finn et al., 2016; Levine et al., 2016). Either the encoder acts to directly recover the underlying states, or simply learns a lower-dimensional embedding where performing reinforcement learning is more straightforward.

Andrychowicz et al. (2020) explore learning to manipulate objects using a mechanical hand using *both* state information from the robot (joint poses, fingertip positions etc) and RGB images. This particular application is an interesting hybrid approach dictated by the domain. State information pertaining to the manipulator is easily obtained, but state information about the pose of the object being manipulated is unavailable and must be recovered using the images. A controller is learned in simulation (MDP), while simultaneously (and separately from the MDP) a separate perception network is learned that maps the image to the pose of the object being manipulated. State information and pose encoding are then concatenated and used as the state vector on which the policy acts. While the pose of the object is unobserved, it is readily recoverable from a single frame (or stack of frames), and hence the partial observation is predominantly a high-dimensional and bijective embedding of the true state. If the true position of the hand was not available, this would be less certain as the object and other parts of the manipulator obfuscates much of the manipulator from any of the three viewpoints (more viewpoints would of course reverse this to being a bijection). The use of a recurrent policy further improves the recovery of state as only the innovation in state needs to be recovered.

### E.2. Asymmetric values

Another well-explored use-case is to instead exploit asymmetric information for to improve learning a value or Q- function (Könönen, 2004; Pinto et al., 2017; Andrychowicz et al., 2020). This is achieved by conditioning either the value function or Q-function on different information than the policy that is either more informative, or lower dimensional representations, and can help guide learning (Könönen, 2004; Pinto et al., 2017). Learning the value or Q function in a lower-dimensional setting enables this function to be learned more stably and with fewer samples, and hence can track the current policy more effectively. Since the value and Q-function are not used at test time, there is no requirement for privileged information to be available when deployed. Pinto et al. (2017) introduce this in a robotics context, using an asymmetric value function, conditioned on the true underlying state of a robotic manipulator, to learn a partially observing agent conditioned only on a third-person monocular view of the arm. Similar ideas were explored previously by Könönen (2004) in relation to semi-centralized multi-agent systems, where each agent only partially observes the world state, but a central controller is able to observe the whole state. The state used by the central controller is used to evaluate the value of a particular world state, whilst each agent only acts on partial information.

### E.3. Behavioral Cloning & Imitation Learning

Behavioral cloning and imitation learning (Kang et al., 2018; Ross et al., 2011), introduced in Main Section 2.3, is, in our opinion, an under-explored avenue for expediting learning in noisy and high-dimensional partially observed processes. The main observation is that this process separates learning to act and learning to perceive (Chen et al., 2020). The fully observing expert learns to act, without the presence of extraneous patterns or noise. The agent then learns to perceive such that it can replicate the actions of the expert. A major benefit of cloning approaches is that perception is reduced to a supervised learning task, with lower variance than the underlying RL task.

Pinto et al. (2017) briefly assess using asymmetric DAgger as a baseline. It is observed that the agent learns quickly, but actually converges to a worse solution than the asymmetric actor-critic solution. This difference is attributed to the experts access to (zero variance) state information otherwise unavailable to the partially observing agent. Our work builds on this observation, seeking to mitigate such weaknesses. Surprisingly, and to the best of our knowledge, no work (including Pinto et al. (2017)) has provided an in-depth analysis of this method, or directly built off this idea.

Chen et al. (2020) showed that large performance gains can be found in an autonomous vehicles scenario by using IL through the use of an asymmetric expert, specifically for learning to drive in the autonomous vehicle simulator CARLA (Dosovitskiy et al., 2017). Chen et al. (2020) train an expert from trajectories, created by human drivers, using behavioral cloning conditioned on an encoded aerial rendering of the environment including privileged information unavailable to the agent at deployment time. The aerial rendering facilitates extensive data augmentation schemes that would otherwise be difficult, or impossible, to implement in a symmetric setting. The agent is then learned using DAgger-based imitation learning. However, this general approach implicitly makes assumptions about the performance of the expert, as well as the underlying identifiability (as we define in Section 4) between the underlying fully and partially observed Markov decision processes.

Other works combine RL and IL to gain performance beyond that of the expert by considering that the expert is sub-optimal (Choudhury et al., 2018; Sun et al., 2018; Weihs et al., 2020), where the performance differential is either as a result of asymmetry, or, the expert simply not being optimal. These works, most often, train a policy that exploits knowledge of the performance differential between the expert and agent, or, the difference in policies. The weight applied to the sample in IL is increased for policies that are similar, or, where the performance gap is small. The example is then down-weighted when it is believed that the expert provides poor supervision in that state. However, these works do not consider updating the expert, and instead focus on ameliorating the drawbacks of AIL using derived statistics. In our work, we seek to define a method for updating an expert directly.

### E.4. Co-learning Expert and Agent

Work that is maybe thematically most similar to ours investigates co-training of the agent and expert. This builds on the AIL approach, where instead of assuming an optimal expert exists, the expert and agent policies are learned simultaneously, where either an additional training phase is added to “align” the expert and agent (Salter et al., 2019; Song et al., 2019), architectural modification (Kamienny et al., 2020), or both (Schwab et al., 2019). An alternative method for deriving such an aligning gradient is to introduce an auxiliary loss regularizing the representation used by the agent to be predictive of the the underlying state, or, a best-possible belief representation (Nguyen et al., 2020).

Salter et al. (2019) trains separate policies for agent and expert using spatial attention, where the expert is conditioned on the state of the system, and the agent is conditioned on a monocular viewpoint. By inspecting the attention map of expert and agent, it is simple to establish what parts of the state or image the policy is using to act. An auxiliary (negative) reward term is added to the reward function that penalizes differences in the attention maps, such that the agent and expert are regularized to use the same underlying features. This auxiliary loss term transfers information from the MDP to the POMDP. The main drawbacks of this approach however are its inherent reliance on an attention mechanism, and tuning the hyperparameters dictating the weight of having a performant agent, expert and the level of alignment between the attention mechanisms. Further, using a attention as the transfer mechanism between the agent and expert somewhat introduces an additional layer of complexity and obfuscation of the actual underlying mechanism of information transfer.

Song et al. (2019) present an algorithm, CoPiEr, that co-trains two policies, conditioned on different information (any combination of fully or partially observing). CoPiEr rolls out under both policies separately, and then selects the rollouts from the policy that performs the best. These samples are then used in either an RL or IL (or hybrid of the two) style update. In this sense, the better performing policy (with ostensibly “better” rollouts) provides high-quality supervision to the policy with lower quality rollouts. MDP to POMDP transfer or privileged information is not considered. Most significantly,



imitation learning is proposed as a method of transferring from one policy to another, or, RL augmented with an IL loss to provide better supervision while retaining RLs capability to explore policy space.

Schwab et al. (2019) on the other hand extend Pinto et al. (2017) by introducing multitask reinforcement learning themes. A “task” is uniquely described by the set of variables that the policy is conditioned on, such as images from different view points, true state information and proprioceptive information. An input-specific encoder encodes each observation before mixing the encoded input features and passing these to a head network which outputs the actions. Instead of aligning attention mechanisms (as per Salter et al. (2019)), Schwab et al. (2019) the head network is shared between tasks providing alignment between the single-input policies. At test time, only those observations that are available need to be supplied to the policy, respecting the partial observability requirement at test time. This approach does not explicitly use an expert, instead using a greater range of more informative information channels to efficiently learn the policy head, while simultaneously co-training the channel-specific encoders.

Finally, the work of Kamienny et al. (2020) present privileged information dropout (PI-D). The general approach of information dropout (Achille & Soatto, 2018) is to learn a model while randomly perturbing the internal state of the model, effectively destroying some information. The hypothesis is that this forces the model to learn more robust and redundant features that can survive this corruption. Kamienny et al. (2020) use this theme by embedding both partial observation and state, where the state embedding is then used to corrupt (through multiplicative dropout) the internal state of the agent. The PI expert is then able to mask uninformative patterns in the observations (using the auxiliary state information), facilitating more efficient learning. The PI can then be easily marginalized out by not applying the dropout term. Importantly however, reinforcement learning is still performed in the partially observing agent, a characteristic we wish to avoid due to the high-variance nature of this learning.